UNIVERSIDADE FEDERAL DO RIO GRANDE DO SUL
INSTITUTO DE CIÊNCIAS BÁSICAS DA SAÚDE
CURSO DE GRADUAÇÃO EM BIOMEDICINA

Camila Kehl Dias

CARACTERIZAÇÃO DE LINHAGEM DE FENÓTIPO DE CICLAGEM LENTA EM MODELO *IN VITRO* DE AGRESSIVIDADE DE MELANOMA HUMANO

Porto Alegre
2019

Camila Kehl Dias

CARACTERIZAÇÃO DE LINHAGEM DE FENÓTIPO DE CICLAGEM LENTA EM MODELO *IN VITRO* DE AGRESSIVIDADE DE MELANOMA HUMANO

Trabalho de conclusão de curso de graduação apresentado ao Instituto de Ciências Básicas da Saúde da Universidade Federal do Rio Grande do Sul como requisito parcial para a obtenção do título de Bacharela em Biomedicina.

Orientador: Prof. Dr. Fábio Klamt

Porto Alegre

2019

CIP - Catalogação na Publicação

Dias, Camila Kehl
Caracterização de linhagem de fenótipo de ciclagem lenta em modelo in vitro de agressividade de melanoma humano / Camila Kehl Dias. -- 2019.
60 f.
Orientador: Fábio Klamt.

Coorientadora: Ivi Juliana Bristot.

Trabalho de conclusão de curso (Graduação) -- Universidade Federal do Rio Grande do Sul, Instituto de Ciências Básicas da Saúde, Curso de Biomedicina, Porto Alegre, BR-RS, 2019.

1. Bioenergética. 2. Câncer de pele. 3. Melanoma. 4. Fenótipo de Ciclagem Lenta. 5. Células Tronco Tumorais. I. Klamt, Fábio, orient. II. Bristot, Ivi Juliana, coorient. III. Título.

Elaborada pelo Sistema de Geração Automática de Ficha Catalográfica da UFRGS com os dados fornecidos pelo(a) autor(a).

Camila Kehl Dias

CARACTERIZAÇÃO DE LINHAGEM DE FENÓTIPO DE CICLAGEM LENTA EM MODELO *IN VITRO* DE AGRESSIVIDADE DE MELANOMA HUMANO

Trabalho de conclusão de curso de graduação apresentado ao Instituto de Ciências Básicas da Saúde da Universidade Federal do Rio Grande do Sul como requisito parcial para a obtenção do título de Bacharela em Biomedicina.

Aprovado em: 04 de julho de 2019.

BANCA EXAMINADORA

_____

Elizandra Braganhol – UFCSPA

_____

Jeferson Franco – UNIPAMPA

_____

Fábio Klamt – UFRGS (orientador)

_____

Ivi Juliana Bristot – UFRGS (coorientadora)

AGRADECIMENTOS

Agradeço à minha mãe a ao meu pai que sempre me apoiaram em todas as minhas ideias mirabolantes e nunca mediram esforços para ver meus sonhos se tornarem realidade. Obrigada por serem os melhores pais que alguém poderia sonhar em ter. Qualquer conquista minha é de vocês também. Da mesma forma agradeço às minhas avós, aos meus avôs e aos meus tios pelo apoio sempre.

Agradeço à Ivi e ao prof. Fábio que me ensinaram tudo que eu sei sobre pesquisa e me inspiram muito. Obrigada por serem meus exemplos científicos e me permitirem participar deste projeto incrível do qual eu tenho muito orgulho. Devo a vocês a pesquisadora que eu sou hoje.

Agradeço também ao Leo e ao Lucas, pessoas que fizeram parte diretamente deste TCC me ajudando nos experimentos. Com certeza este trabalho não seria o mesmo sem vocês, obrigada de coração.

Agradeço ao pessoal do laboratório 24F, Lúcia, Henrique, Dai, Pati, Maria, Cássio, Jéssica, Lia por todas as risadas, pela ajuda e pelo apoio nos momentos difíceis. Vocês são os melhores colegas de laboratório e amigos que alguém poderia pedir.

Agradeço ao Guilherme, meu namorado, pelo apoio incondicional. Por estar sempre ao meu lado e me ajudar sempre. Obrigada por absolutamente tudo.

Agradeço à Marília, minha colega de formatura e amiga, sem ela meus anos de faculdade de Biomedicina não teriam sido os mesmos com certeza. Obrigada pelas noites de estudo e pela amizade.

Por fim, agradeço a UFRGS e aos professores que me tornaram a profissional que eu sou hoje! Sou muito grata.

RESUMO

O melanoma é um tipo de câncer de pele que se origina dos melanócitos, células produtoras de melanina. A incidência excessiva de luz UV sobre a pele é o maior fator de risco para o desenvolvimento desta doença. No Brasil, o melanoma é o câncer de pele que apresenta maior taxa de mortalidade, quando comparada à taxa de incidência. Especialmente após o processo de metástase, é um dos cânceres que mais apresenta resistência ao tratamento. O fenótipo de ciclagem lenta é um assunto que tem sido bastante abordado na literatura dos últimos anos e que, juntamente com o modelo de células tronco tumorais, visa explicar como a heterogeneidade tumoral gera respostas distintas a estímulos iguais no câncer. Neste trabalho, um modelo de agressividade de melanoma humano *in vitro* foi utilizado para explorar características do metabolismo e ciclo celular de quatro linhagens celulares de melanoma. Três linhagens foram obtidas a partir da linhagem celular A375, chamadas A7, G10 a PCDNA3. Foi observado que as linhagens apresentam taxas diferentes de crescimento e os parâmetros da respiração mitocondrial avaliados também apresentaram diferenças entre as linhagens. Algumas características da linhagem G10 como seu metabolismo altamente oxidativo, resistência ao tratamento com carboplatina e maior atividade de um marcador de senescência indicam que esta linhagem faz parte do fenótipo de ciclagem lenta. Uma linhagem em específico, G10, pode ser classificada como um fenótipo de ciclagem lenta. Propomos que este modelo pode ser aplicado no estudo do melanoma humano como um modelo de heterogeneidade tumoral e que a linhagem G10 é uma linhagem enriquecida em células do fenótipo de ciclagem lenta.

Palavras-chave: Bioenergética. Câncer de pele. Melanoma. Fenótipo de Ciclagem Lenta. Células Tronco Tumorais.

ABSTRACT

Melanoma is a type of skin cancer that originates from melanocytes, melanin-producing cells. The excessive incidence of UV light on the skin is the most important risk factor for the development of this disease. In Brazil, melanoma is the type of skin cancer that presents the highest mortality rate, when compared to the incidence rate. Especially after the metastasis process, it is one of the most resistant cancers to treatment. The slow-cycling phenotype is a subject that has been widely discussed in the literature of recent years and, together with the cancer stem cell model, aims to explain how tumor heterogeneity generates distinct responses to equal stimuli in cancer. In this work, an *in vitro* human melanoma aggressiveness model was used to explore cell metabolism and cell cycle characteristics of four melanoma cell lines. Three lines were obtained from the A375 cell line, called A7, G10 to PCDNA3. It was observed that the lineages present different growth rates and the mitochondrial respiration parameters evaluated presented differences between the lines. Some characteristics of the G10 lineage such as its highly oxidative metabolism, resistance to carboplatin treatment and increased activity of a senescence marker indicate that this lineage is part of the slow-cycling phenotype. Specifically the G10 cell line, can be classified as a slow-cycling phenotype. We propose that this model can be applied in the study of human melanoma as a model of tumor heterogeneity and that the G10 cell line is enriched in slow-cycling phenotype cells.

Keywords: Bioenergetics. Skin cancer. Melanoma. Slow-cycling phenotype. Cancer Stem Cells.

LISTA DE FIGURAS

SUMÁRIO

1 INTRODUÇÃO COMPREENSIVA

Neste trabalho é abordada a relação entre níveis de agressividade diferenciais de um modelo *in vitro* de melanoma humano com suas respectivas características bioenergéticas e ciclo celular. Alguns assuntos relevantes para o melhor entendimento do modelo de estudo e dos resultados obtidos e suas implicações são discorridos abaixo.

1.1 CÂNCER

De acordo com o Instituto Nacional do Câncer (INCA) o câncer é considerado como um conjunto de doenças em que ocorre o crescimento desenfreado de células de forma anormal, resultando em tumores que podem ser benignos ou malignos. Tumores malignos podem evoluir para metástase, quando as células neoplásicas migram para outros lugares que não o lugar de início do desenvolvimento da doença. No Brasil, o câncer é o segundo tipo de doenças crônicas não transmissíveis com maior taxa de mortalidade (MINISTÉRIO DA SAÚDE, 2016).

De acordo com o National Cancer Institute (NIH, Estados Unidos) o câncer se forma a partir do acúmulo de inúmeras mutações em genes específicos. Essas são selecionadas pelo microambiente tumoral de forma a desenvolver-se em um tumor maligno constituído de diferentes populações celulares em diferentes estágios de evolução; o que dificulta as estratégias de tratamento e eliminação completa do câncer (GILLIES; VERDUZCO; GATENBY, 2012; TABASSUM; POLYAK, 2015). Alguns fatores reconhecidamente necessários para o estabelecimento do câncer podem ser listados como: mutações e instabilidade genômicas, perda da limitação de replicação, manutenção da sinalização proliferativa, evasão de supressores de crescimento, evasão do sistema imune, indução de angiogênese, promoção da inflamação tumoral, resistência a morte celular, desregulação da bioenergética celular e ativação de vias de invasão e metástase (HANAHAN; WEINBERG, 2011).

1.1.1 Melanoma

A incidência de radiação UV na pele é o maior fator de risco para desenvolvimento do melanoma; sendo esta doença uma proliferação exagerada de melanócitos, células produtoras de melanina que podem ser estimuladas a proteger a pele da incidência solar (GILCHREST et al., 1999; LEONARDI et al., 2018; PENNELLO; DEVESA; GAIL, 2000). O melanoma é

conhecido por ser resistente às terapias convencionais, como quimioterapia e radioterapia (FISCHER et al., 2018). De acordo com dados de 2017 mais de 80% das mortes devidas a cânceres de pele são referentes a casos de melanoma (SIEGEL; MILLER; JEMAL, 2017). De acordo com a Organização Mundial de Saúde (WHO) em 2018 foram registrados 559.371 novos casos de câncer no Brasil, dos quais 7.407 foram casos de melanoma. Segundo o INCA e o Ministério da Saúde a razão incidência/mortalidade para cânceres de pele não melanoma é de 90.3 para homens e 145.7 para mulheres, enquanto para melanoma está taxa cai para 4.2 para homens e 5.6 para mulheres. Quanto menor a razão incidência/mortalidade pior o prognóstico, sendo influenciada por características de malignidade dos tumores. Especialmente para melanomas de estágio 4, quando já há metástase, o prognóstico ainda é muito ruim devido à crescente resistência observada. Os tratamentos mais acreditados atualmente envolvem combinação de inibidores dos oncogenes *MEK* e *BRAF* e imunoterapia, porém os resultados indicam apenas melhora parcial na sobrevivência dos pacientes (CHAPMAN et al., 2011; HODI et al., 2010; VERDUZCO; FLAHERTY; SMALLEY, 2015).

1.1.1.1 Metabolismo do melanoma

No câncer a glicólise pode atuar como rota principal de obtenção de energia e o piruvato é convertido à lactato para renovar o NAD+ celular (WARBURG, 1956). Nesse caso o metabolismo é desviado de forma a utilizar o carbono do piruvato e seus intermediários para a produção de moléculas que suportem a rápida divisão celular, em contrapartida a oxidação destes carbonos na fosforilação oxidativa (NELSON; COX, 2008). Por isso há uma relação, a respeito do estado metabólico em melanomas, de células de melanoma com mutação em BRAF que são altamente dependentes da glicólise e este perfil está mais ligado a tumores benignos (ABILDGAARD; GULDBERG, 2015; HALL et al., 2013). Esse fenótipo condiz com a teoria de Otto Warburg de que toda célula tumoral apresentaria um fenótipo glicolítico e de ciclagem rápida (SCOTT et al., 2011). Em contrapartida o perfil mais dependente da fosforilação oxidativa para produção de ATP, relacionado ao fenótipo de ciclagem lenta, é relacionado a resistência ao tratamento e metástases em melanomas (AHN; CHATTERJEE; ECCLES, 2017a). Estas células optariam por manter o piruvato no ciclo do ácido cítrico e oxidá-lo a CO_2 via fosforilação oxidativa. Dessa forma não haveria tanto suporte para a rápida duplicação celular como no caso das células “viciadas” em glicólise (ABILDGAARD; GULDBERG, 2015; NELSON; COX, 2008). Além disso, células de melanoma com a mutação BRAF também já foram relacionadas a um fenótipo altamente oxidativo e, indiretamente, a diminuição da

expectativa de sobrevivência de pacientes (FISCHER et al., 2018). Já foi visto que células de melanoma podem ser mais glicolíticas que melanócitos, mas que também podem se adaptar seu metabolismo de forma mais eficiente às mudanças do ambiente (SCOTT et al., 2011).

Já foi observado que apenas 35 a 50% das linhagens celulares com mutação em *BRAF* ou do fenótipo *wild-type* podem ser caracterizadas como *high-OXPHOS* (GOPAL et al., 2014; HAQ et al., 2013; ZHANG et al., 2016). Este fenótipo altamente oxidativo está relacionado a maior atividade de diversas proteínas, dentre elas *mTORC1* e, consequentemente, *MYC* e *HIFα* (SHIMOBAYASHI; HALL, 2014). Entretanto, também deve-se considerar que a produção intensa de lactato realizada pelas células em glicólise anaeróbia podem contribuir para o microambiente tumoral, que leva a seleção de células mais resistentes (PINHEIRO et al., 2016).

1.1.1.2 Linhagem A375 e clones derivados

A linhagem A375 de melanoma maligno amelanocítico e seus clones derivados foram utilizados nesse trabalho como modelo de agressividade. A linhagem A375 possui a mutação $BRAF^{V600}$, presente em 50% dos melanomas metastáticos (PARMENTER et al., 2014). Esta linhagem foi transfectada com cDNA de catalase no vetor pcDNA3 dando origem às linhagens A7 e G10, e à linhagem PCDNA3 transfectada com o vetor vazio. A linhagem A7 apresenta genes da via da melanogênese, normalmente *downregulated* em melanomas agressivos, *upregulated*; assim como genes relacionados a adesão celular. Enquanto a linhagem G10 apresenta genes associados a melanomas agressivos *upregulated*, assim como genes anti-apoptose, de processos de metabolismo de drogas e da via de sinalização ErbB (BRACALENTE et al., 2016a). Tanto A7 quanto G10 apresentam ativação das cinases ERK 1/2 diminuída em relação à controle PCDNA3, mas apenas A7 apresentou diminuição da atividade de Akt em relação à controle. ERK ½ e Akt fazem parte de vias de sinalização responsáveis por alteração na resposta de sobrevivência e crescimento a estímulos externos. Além disso, na linhagem A7 houve a reversão de características malignas por apresentar maior expressão da proteína TYRP1, reativando a via da melanogênse nesse clone e a produção de melanina, gerando tumores pigmentados. Diferentemente, como visto na Figura 1, a linhagem G10 apresentou maior nível de desdiferenciação em sua morfologia e maior capacidade demigração, além de ser o único dentre os quatro clones capaz de causar metástase em camundongos *Nude* xenoimplantados (BRACALENTE et al., 2016b). Além disso, já foi observado que a linhagem G10 apresenta maiores níveis de cofilina-1, proteína mediadora da polimerização da actina e migração celular. A cofilina-1 já foi demonstrada como biomarcador

de malignidade em melanomas, sendo correlacionada a um pior prognóstico (BRACALENTE et al., 2018).

Figura 1 – Crescimento diferencial dos xenoimplantes das quatro linhagens.

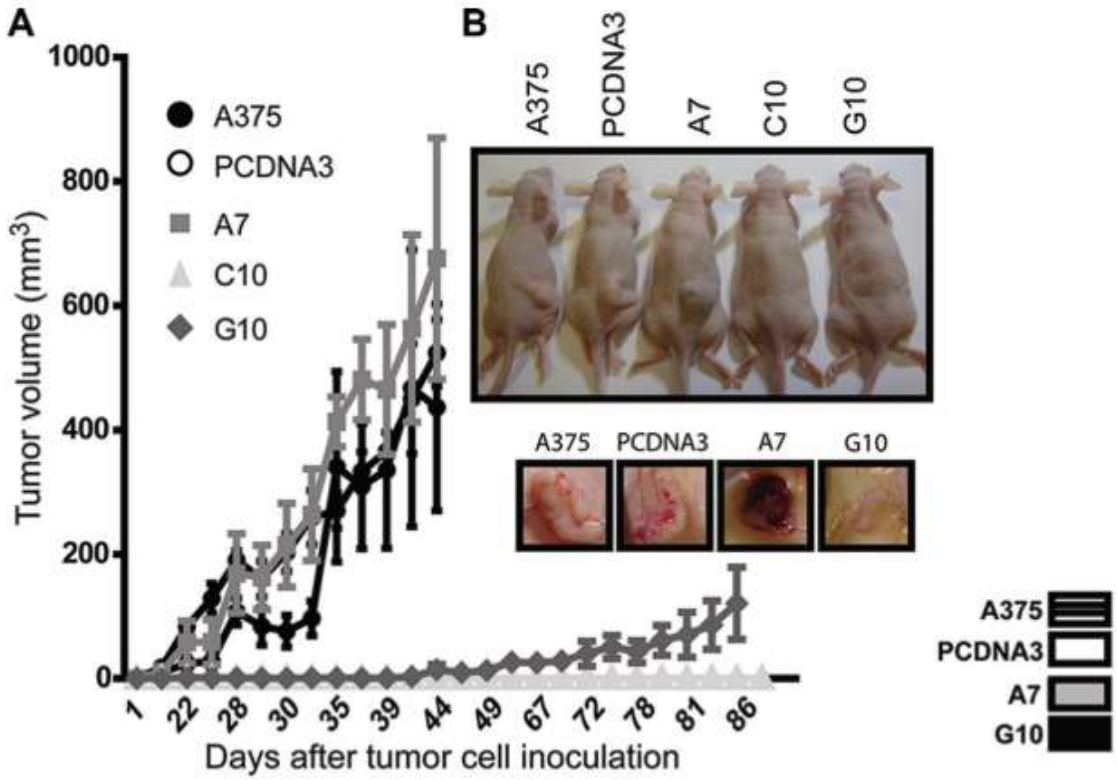

Xenoimplantes das linhagens A375, PCDNA3, A7 e G10 em camundongos *Nude*, em detalhe, tumores visivelmente distintos referentes ao xenoimplante de cada linhagem.
Fonte: BRACALENTE et al., (2016b).

1.2 HETEROGENEIDADE E EVOLUÇÃO TUMORAL

A teoria da evolução tumoral leva em conta que a busca pelo entendimento do porquê um fenótipo específico de câncer é capaz de se estabelecer como doença, e outros não, deve visar além do genótipo e da procura por mutações específicas causadoras do câncer (ADJIRI, 2017). Constantemente as células de uma população tumoral são selecionadas pelo microambiente tumoral em formação por processos como acidose e hipóxia e é necessário levar em consideração que os processos evolutivos intratumorais selecionam o fenótipo e não o genótipo. Essa seleção intratumoral do microambiente também propicia o surgimento de populações de células muito bem adaptadas, ao mesmo tempo, e podem vir a ser responsáveis pela resistência à terapia. Dessa forma o tratamento atua como um agente de seleção epigenética e genética em tumores (GILLIES; VERDUZCO; GATENBY, 2012).

No início dos estudos sobre a biologia celular de tumores acreditava-se que um tumor evoluía a partir de uma única célula, a partir de determinadas mutações, e que todo o tumor formado após era derivado da expansão clonal desta única célula. Acreditava-se que as células do tumor poderiam divergir entre si devido ao acúmulo de mutações, porém que sua origem permanecesse a mesma (NOWELL, 1976). Na atualidade já se sabe que um tumor pode ter diferentes respostas a uma gama de estímulos devido a heterogeneidade das células que o compõem, que não necessariamente surge da variabilidade genética (MCGRANAHAN; SWANTON, 2015b). Isto pode ser exemplificado pela observação de uma resposta desigual ou inesperada a um tratamento com certo quimioterápico, por exemplo. Sendo assim, a heterogeneidade tumoral é caracterizada pela heterogeneidade funcional e fenotípica entre os grupos de células que compõem um tumor (HEPPNER, 1984). Devido a presença de diversas populações em um mesmo tumor também já foram observadas interações entre as diferentes populações. Estas interações podem ser tanto competitivas, qual população é mais adaptada ao ambiente, quanto sinérgicas, uma população produz algum fator que a outra necessita, por exemplo (GATENBY; CUNNINGHAM; BROWN, 2014). Dessa forma vários resultados podem ser esperados, sem que as interações intratumorais em cada caso sejam conhecidas. Assim como as terapias aplicadas atualmente podem suscitar diferentes respostas tumorais. A terapia aplicada pode eliminar apenas as células que consomem muitos nutrientes e limitam o crescimento do tumor, levando a uma regressão inicial; porém o tumor voltará a crescer sem a presença das células "limitantes", como exemplificado na Figura 2(TABASSUM; POLYAK, 2015).

Figura 2 – Exemplo de tratamentos que não contemplam a heterogeneidade tumoral.

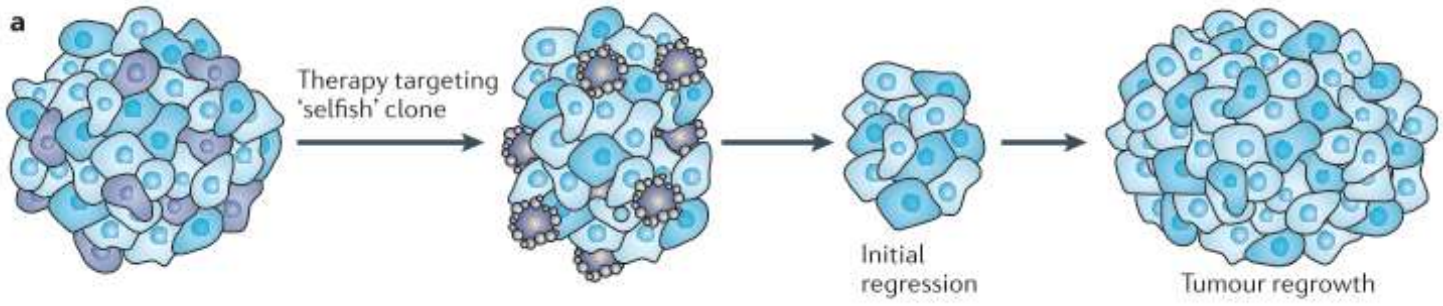

Exemplo de tratamentos que não contemplam a heterogeneidade tumoral, não contribuindo para a eliminação do tumor de fato.
Fonte: TABASSUM; POLYAK (2015).

1.3 REPROGRAMAÇÃO METABÓLICA NO CÂNCER

Além do acúmulo de mutações, outro fator necessário para o estabelecimento desta doença é a reprogramação metabólica. É comprovado que alterações na bioenergética celular são cruciais para atendimento das demandas energéticas do câncer e estabelecimento da doença (HANAHAN; WEINBERG, 2011). Células do câncer que se multiplicam rapidamente e requerem grandes quantidades de substrato para diversas rotas de biossíntese realizam a glicólise anaeróbica descrita por Otto Warburg em 1930. A partir do efeito Warburg o metabolismo do câncer, em geral, foi definido como a preferência por converter piruvato a lactato e realizar a chamada glicólise aeróbica, ao invés de oxidar o piruvato e gerar uma maior quantidade de ATP (VANDER HEIDEN; CANTLEY; THOMPSON, 2009). Entretanto, o que tem sido evidenciado na literatura é que em um tumor podem haver diferentes subpopulações que apresentam estados bioenergéticos distintos.

Desta forma a correlação entre células de câncer que apresentam fenótipo de ciclagem lenta e resistência a terapias e ocorrência de metástases já foi descrita e é um problema crescente no manejo desta doença. Isto devido a maior parte das terapias terem como alvo células de ciclagem rápida cujo metabolismo segue o efeito Warburg (AHN; CHATTERJEE; ECCLES, 2017a; ROESCH et al., 2013). Porém a heterogeneidade tumoral contribui para que após o tratamento comum apenas algumas células do tumor sejam eliminadas e outras, mais resistentes e não atingidas pelo tratamento, perdurem, podendo causar metástases (TABASSUM; POLYAK, 2015).

1.3.1 Fenótipos de ciclagem lenta

Fenótipos de ciclagem lenta vêm sendo mencionados na literatura por contradizerem o efeito Warburg, no sentido que são fenótipos observados em células de câncer que apresentam metabolismo oxidativo (ROESCH et al., 2013). Portanto, estas células realizariam a oxidação do piruvato via fosforilação oxidativa, diferentemente do que foi descrito por Warburg. Considerando que a maioria das terapias disponíveis como quimioterapia e radioterapia têm por definição foco em atingir células de ciclagem rápida, vemos que a atual forma de tratamento apenas selecionaria as populações de células de ciclagem lenta e/ou células tronco tumorais (BLAGOSKLONNY, 2005). Portanto a mudança de perfil metabólico e as características apresentadas pelo fenótipo de ciclagem lenta estão associadas à resistência ao tratamento e ao alto potencial de formação de novos tumores e metástases (AHN; CHATTERJEE; ECCLES,

2017a). Outro fator importante é a descrição de características senescentes aliadas ao fenótipo de ciclagem lenta e à resistência ao tratamento (SUN et al., 2014). Alguns marcadores que definiriam estas populações de ciclagem lenta já foram identificados como a expressão aumentada do gene *JARID1B*. Esse gene codifica uma histona demetilase, que faz parte de uma família de demetilases associadas ao desenvolvimento de tecidos, câncer e biologia de células tumorais (DEY et al., 2008). O fenótipo *JARID1B*^{high} já foi observado em melanomas, porém apenas pelo isolamento, a partir de uma linhagem celular, de uma população de células que apresenta o fenótipo e outros marcadores (PEREGO et al., 2018; ROESCH et al., 2013). Além disso, os fenótipos de ciclagem lenta já foram comparados às células tronco tumorais do modelo que visa explicar a heterogeneidade tumoral (KONRAD et al., 2016).

1.3.2 Senescência

Células senescentes são caracterizadas por apresentaram baixos níveis proliferativos dentre outras mudanças metabólicas que geram um fenótipo "dormente" (LEE; SCHMITT, 2019). Este processo decorre principalmente devido ao processo de *aging* e da diminuição de telômeros (SHAY, 2016). Ativação de certos oncogenes, expressão de algumas citocinas e produção de espécies reativas de oxigênio são fatores que podem resultar em um tipo de senescência prematura induzida por estresse (KUILMAN et al., 2010). A senescência é um recurso disponível para células tumorais, especialmente como desvio de outra forma de saída do ciclo celular, a apoptose; pois, as células senescentes permanecem viáveis por mais tempo e exibem um padrão secretório característico (COPPÉ et al., 2010). Sendo assim, quando uma população de células de câncer é submetida a doses subletais de um quimioterápico essas células podem entrar em senescência, já que processos de evasão de morte celular podem estar ativos no câncer, e não prosseguirão para a próxima fase do ciclo celular. Estas células podem entrar em um estado de senescência induzido por terapia, associado a mudanças morfológicas e no metabolismo (EWALD et al., 2010; GEWIRTZ, 1999). Populações senescentes podem resistir ao tratamento e voltar ao ciclo celular após o mesmo, causando a reincidência do câncer e consequências graves aos pacientes (HSU; ALTSCHULER; WU, 2019). Um importante mediador dos processos de senescência induzida por terapia é o inibidor de cinase dependente de ciclina (CDKN1A), gene p21 (ABBAS; DUTTA, 2009; CAZZALINI et al., 2010).

1.4 JUSTIFICATIVA

Este trabalho contribuiu para a pesquisa na área de estudo do câncer pois traz conceitos de metabolismo tumoral associados ao fenótipo inovadores, por meio da caracterização de um modelo celular de agressividade gerado a partir de células de uma única linhagem tumoral. Além disso foca na heterogeneidade de fenótipos presente no modelo e a diferença crítica entre a velocidade de ciclagem de cada linhagem e como isso afeta o fenótipo observado. Também estabelece uma potencial linhagem enriquecida em células de ciclagem lenta, algo ainda não descrito na literatura.

1.5 OBJETIVOS

Visamos caracterizar o metabolismo de um modelo celular de agressividade de melanoma humano, já descrito previamente, de modo a obter um modelo que contemple a heterogeneidade tumoral. Buscamos relacionar mudanças no metabolismo energético (oxidativo ou glicolítico) e nível de agressividade de linhagens celulares com fenótipos de ciclagem lenta ou rápida. Com isso também visamos a caracterização de uma linhagem permanentemente enriquecida com células de ciclagem lenta.

1.5.1 Objetivo geral

Avaliar se há relação entre a bioenergética, nível de agressividade e velocidade de ciclagem de um modelo *in vitro* de melanoma humano.

1.5.2 Objetivos específicos

São objetivos específicos deste trabalho:

a) avaliar o tempo de duplicação das linhagens do modelo;
b) avaliar a resposta das linhagens a quimioterápicos;
c) estabelecer mudanças no perfil das fases do ciclo celular em cada linhagem;
d) avaliar a ocorrência de senescência.

2 ARTIGO CIENTÍFICO

Characterization of a slow-cycling phenotype enriched cell line in *in vitro* aggressiveness melanoma model.

Camila K. Dias [1], Ivi J. Bristot [1], Leo M. Martins [1], Lucas K. Grun [1], Fátima C. R. Guma [1], Florencia Barbé-Tuana [2], Hebe Durán [3], Fábio Klamt [1]

1 Laboratory of Cellular Biochemistry, Department of Biochemistry, Universidade Federal do Rio Grande do Sul, Porto Alegre 90035-000, Brazil
2 Department of Immunology, Pontifícia Universidade Católica do Rio Grande do Sul, Porto Alegre 90619-900, Brazil
3 Consejo Nacional de Investigaciones Científicas y Tecnológicas, Buenos Aires C1425FQB, Argentina

Corresponding Author: Camila Kehl Dias
E-mail adress: camila.kehldias@gmail.com
Department of Biochemistry, Universidade Federal do Rio Grande do Sul, Porto Alegre 90035-000, Brazil

ABSTRACT

The slow-cycling phenotype is an emerging issue in the study of cancer, especially in melanoma. Together with the Cancer Stem Cell (CSC) model, this cellular phenotype presents a slower growth rate, greater treatment resistance and metastasizing potential. CSCs also present the capacity to originate all populations in a tumor and can alternatively present dormant behavior, contemplating tumor heterogeneity. Here we present a cell panel derived from amelanocytic melanoma A375 cell line, with differential aggressiveness levels and explore its bioenergetics and cell cycling states. The G10 cell line, the most aggressive clone, presented high-OXPHOS metabolism and slow-cycling phenotype characteristics, such as resistance to carboplatin and plastic growth rate. These features might be driven by cell cycle arrest to G0/G1 phases, as well as higher p21 expression. Additionally, the G10 cell line presents higher activity of the senescent marker SA-β-galactosidase. This study presents a cell panel composed of four cell lines which can represent tumor heterogeneity in a study model, including a slow-cycling enriched cell line.

KEYWORDS: Bioenergetics/Cancer Stem Cells/Melanoma/Slow-Cycling Phenotype/Skin Cancer.

INTRODUCTION

Melanoma is considered to be any malignant lesion originated from melanocytic neoplasms (Shain & Bastian, 2016). Excessive exposure to ultraviolet (UV) light radiation from the sun is considered as the main cause for development of melanoma skin cancer (Gilchrest *et al*, 1999; Leonardi *et al*, 2018; Pennello *et al*, 2000). In Brazil non-melanoma skin cancer is the most incident, on the other hand melanoma is less incident but more lethal (Brazil, 2018). In 2018, 287,723 new cases of skin melanoma and 60,712 deaths due to this disease worldwide were reported (Bray *et al*, 2018). Melanocytes go through a metabolic reprogramming process whilst becoming melanoma, these alterations support the tumor metabolism and are crucial to cancer development (Verduzco *et al*, 2015; Hanahan & Weinberg, 2011). According to the Warburg effect theory cancer cells should present a more glycolytic metabolism and high production of lactate (Vander Heiden *et al*, 2009). Some melanoma study models do in fact present this glycolysis "addicted" phenotype (Bettum *et al*, 2015; Hall *et al*, 2013), however there have been some melanoma model phenotypes characterized as "High-OXPHOS"(Gopal *et al*, 2014). In addition, it has been considered that focusing on the phenotypes that thrive during tumor progression might be more important than focusing on tumor driving mutations and genotype (Adjiri, 2017; Gillies *et al*, 2012).

It is still partially unknown why cancer responds in such heterogeneous form to treatment and what mechanisms select the set of cell populations comprehended in a single tumor (Tabassum & Polyak, 2015). However, the slow-cycling phenotype emerges as a possibility of explanation for this phenomenon and sets a course to the better understanding of tumor evolution and dynamics (Ahn *et al*, 2017). Besides the obvious lower duplication rate, other characteristics have been associated to the slow-cycling phenotype in melanomas: highly oxidative metabolic profile, higher tumor aggressiveness and resistance to oxidative stress and treatment (Ahn *et al*, 2017; Fischer *et al*, 2018; Roesch *et al*, 2013; Vazquez *et al*, 2013). Many works have already proposed some molecular markers that might be associated to the slow-cycling phenotype and its presence within cancer study models. Some of these markers include higher expression of the *JARID1B* gene, a histone demethylase, higher levels of senescence markers and cell cycle arrest in response to treatment (Roesch *et al*, 2013, 2010; Ravindram Menon *et al*, 2015; Webster *et al*, 2015).

Nonetheless, another concept has been consistently brought up is the Cancer Stem Cells (CSC) model, which was also created in order to explain tumor heterogeneity and progression (Reya *et al*, 2001; Shackleton *et al*, 2009). In fact, the CSC model has been a title of discussion for quite a while before the slow-cycling phenotype (Hamburger & Salmon, 1977). The CSC model comprises a list of characteristics that would define a cancer stem cell, such as the presence of an undifferentiated population of cells in a tumor and the poorer prognosis coupled with it (Morrison *et al*, 2012). The CSC model focus on the self-renewal capacity of the common stem cell and how this trait is crucial for cancer development. However, the similarity between the CSC model and the slow-cycling phenotype is critical, to a point where this difference can become indistinguishable (Konrad *et al*, 2016; Visvader & Lindeman, 2008; Morrison *et al*, 2012).

Despite extensive study over the slow-cycling phenotype together with the CSC model in cancer and in melanomas, a slow-cycling cell line has not been reported yet. A melanoma aggressiveness cell model has been developed by Bracalente and colleagues with the A375 human amelanocytic melanoma cell line and its derived clones PCDNA3, control of transfection, G10 and A7, which were transfected with the catalase gene (Bracalente *et al*, 2016a, 2016b). The G10 cell line presents higher aggressiveness when compared to the others. When Nude mice were inoculated with each cell line, the G10 tumor growth rate was much lower but was the only cell line capable of metastasis. On the other hand the A7 cell line presented benign melanoma traits, such as activation of the melanogenesis pathway (Bracalente *et al*, 2016b). Moreover it has been reported that the G10 cell line presents higher cofilin-1 levels, which has been associated with poorer prognosis in melanoma (Bracalente *et al*, 2018).

In this work, we aimed on characterizing the G10 cell line as a potential slow-cycling enriched cell line. Only recently light has been shed over the slow-cycling phenotype and there is still much to be understood of it. We also aimed on identifying differences in the cellular bioenergetics and biomarkers on the cell panel comprising A375, PCDNA3, A7 and G10. In this sense, the aggressiveness cell model composed of the four human melanoma cell lines presents potential as a study model comprehending diverse phenotypes and representative of tumor heterogeneity.

RESULTS

G10 cell line presents High-OXPHOS phenotype

Firstly, the respiratory curves determined by High Resolution Respirometry (HRR) analysis were different between the cell lines A375, A7, G10 and PCDNA3. Therefore, each cell line presents a unique respiratory profile. Oligomycin was used to inhibit ATP-synthase activity to establish the ATP-linked respiration, as well as the LEAK respiration, which corresponds to the proton leak between the intermembranes space and the mitochondrial matrix. The carbonyl cyanide-4-(trifluoromethoxy)phenylhydrazone (FCCP) ionophore was used to dissipate the proton gradient and observe maximum ETS (Electron Transfer System) capacity of the mitochondria in each cell line. Finally, rotenone was used to inhibit complex I (NADH reductase) activity and antimycin A was used to inhibit complex III (cytochrome oxidase) activity, both mitochondrial poisons used to establish the residual oxygen consumption (ROX).

Taking a closer look at each aspect of the mitochondrial respiration, we observed that G10 cell line presented a significantly higher basal oxygen consumption rate (OCR) and higher LEAK respiration when compared to all other cell lines. The respiration linked to ATP-synthesis (also known as coupled respiration) was higher for G10 when compared to A7 only. The same pattern was observed for the maximum respiration or maximum electron transfer capacity achieved when the ETS in the respiratory chain is uncoupled from ATP-synthesis. Reserve capacity was diminished in A7 and G10 when compared to PCDNA3. After complete blocking of the mitochondrial respiration with rotenone and antimycin A the ROX respiration is observed, where G10 and A7 cell lines presented elevated ROX when compared to the control cell lines A375 and PCDNA3. Altogether the G10 cell line presented more oxidative metabolism when compared to the other cell lines, taking into account that all respiratory aspects observed here were augmented in this cell line.

The G10 cell line presents irregular doubling time

To determine the doubling time of each cell line, growth curves were assembled using data from different initial cell densities (1.000, 2.000, 4.000 and 8.000 cells) for a 96 hours period. It was possible to obtain replicable doubling times for A375 (16,3 hours), A7 (20,9 hours) and

PCDNA3 (14,6 hours) cell lines. A7 doubling time was significantly higher when compared to A375 and PCDNA3. Because G10 doubling time varied considerably with initial cell density plated we tested data variance homogeneity. Applying the test to the whole data set resulted in a significant *p* value for the variance homogeneity test, the same did not occur when we applied the test to a data set containing only A375, A7 and PCDNA3 data. Therefore, G10 does not present a constant doubling time. It appears that the G10 cell line is capable of adjusting its growth and delaying population duplication when necessary (high cell density).

Cell cycle phases distribution profiles

We found that the A375 cell line presented a polyploid profile with 4n cells, which can be seen in Figure 6 as the third peak in yellow making. The cell cycle analysis revealed a concentration of the G10 cell line cells on G0/G1 when compared to all other cell lines. Moreover, the A7 and PCDNA3 cell lines presented more cells in G0/G1 than A375. Concerning the S phase, A375 cell line presented the lesser amount of cells in S phase and PCDNA3 the greater. A7 and G10 cell lines did not present differences in amount of cells on S phase. Moving over to the G2 phase, A375 presented the greater amount of cells on G2 phase when compared to all others. Finally, G10 presented the lesser amount of cells on G2 phase when compared to all other cell lines, leading to the conclusion that this cell line presented the most different cell cycle profile with G0/G1 arrest.

Senescence-associated *β*-galactosidase activity is different throughout the cell panel

As a cellular parameter of senescence, we determined the activity of the senescence-associated *β*-galactosidase (SA-*β*-gal) enzyme by flow cytometry. The results are shown in Mean Fluorescence Intensity (MFI) generated from cleavage of 5-dodecanoylaminofluorescein di-*β*-D-galactopyranoside (C_{12}FDG), a *β*-galactosidase substrate that is modified to include a 12-carbon lipophilic moiety. Once inside the cell, the substrate is cleaved by *β*-galactosidase producing a fluorescent product that is well retained by the cells and can represent the activity of SA-*β*-galactosidase. The G10 cell line presented the highest SA-*β*-gal activity. There was no difference of this enzyme activity when comparing A375, A7 and PCDNA3.

Differential p21 gene expression

Previous gene expression data from a microarray RNA chip obtained by Bracalente and colleagues (Bracalente *et al*, 2016a) permitted the evaluation of p21 (*CDKN1A* - Cyclin Dependent Kinase Inhibitor 1) gene expression levels. The p21 gene has been reported to be

imperative for senescent cells in viability mantainance (Yosef *et al*, 2017). Differential expression of p21 amongst the cell panel indicates that the G10 cell line presents higher expression of p21 when compared to all other cell lines.

Cell lines respond differentially to treatment with carboplatin

The melanoma cell lines were treated with carboplatin doses ranging from 5 μM to 150 μM for 72 hours to obtain the GI50 (dose that cause 50% growth inhibition) for A375 (55.88 μM), PCDNA3 (53.47 μM), A7 (58,09 μM) and G10 (111.96 μM). G10 cell line presented GI50 dosage approximately two fold higher than all other cell lines. G10 was the only cell line to present statistically significant difference in response to treatment with carboplatin.

DISCUSSION

Overall, our results indicate that the aggressiveness cell model studied here presents cell lines that diverge in metabolic profiles and cell cycle patterns. The G10 cell line presents a high-OXPHOS phenotype and appeared to be resistant to carboplatin treatment. Along with these characteristics other important indications of G10 being a slow-cycling enriched cell line were observed. The G10 cell line presented G0/G1 arrest, which lead us to seek an explanation to this cell cycle arrest. In this sense, we observed that the G10 cell line presents higher activity of the senescence-associated *β*-galactosidase and higher p21 expression when compared to all other cell lines. Here we show that the G10 cell line is enriched in slow-cycling phenotype cells, which could be due to increased activation of senescent processes.

It has been well established that intratumoral heterogeneity is the main reason for cancer resistance to treatment (Greaves, 2015). Better strategies must be applied in the study of how cancer can evade all kinds of treatment developed so far if the final goal is to apply better strategies in patient care, especially concerning intratumoral heterogeneity (McGranahan & Swanton, 2017, 2015). Taking that into account our aim here was to present and explore a cell panel that is heterogeneous in metabolism and response to treatment, amongst other aspects. This cell panel presents as a promising study model since A7, G10 and PCDNA3 are derived from A375 cell line and all differences reported here are due to the phenotypical changes caused

by catalase transfection (PCDNA3 control of transfection). The *in vitro* model also presents differential levels of aggressiveness which contributes to the heterogeneity of response (Bracalente *et al*, 2016b, 2018). Additionally, in this work, we describe the first cell line that is permanently enriched in slow-cycling cells. The slow-cycling phenotype has gained much strength in being, probably, an important factor for resistance to treatment in melanoma and in other cancers (Ahn *et al*, 2017; Roesch *et al*, 2010; Perego *et al*, 2018; Hoang-Minh *et al*, 2018).

Firstly, based on HRR data, we showed that the G10 cell line presents a High-OXPHOS phenotype, as seen in Fig. 1 and Fig. 2, when compared to all other cell lines of the panel. All respiratory parameters evaluated here were enhanced for the G10 cell line, except for the reserve capacity (Fig. 2). The lower reserve capacity together with higher proton leak respirations suggests some level of overwork of the mitochondria in this cell line, it can also mean that respiration is not fully coupled with ATP-synthesis or indicate some damage to the mitochondria (Fig. 1). Additionally, it is possible to infer that A375, PCDNA3 and A7 cell lines depend more on glycolysis considering the lower respiratory rates found (Figure 1 and 2). This corroborates with findings in melanoma and other cancers which correlate the highly oxidative phenotype with aggressive characteristics (Hoang-Minh *et al*, 2018; Roesch *et al*, 2013). Highly oxidative metabolism is associated with elevated activity of the PGC1α pathway, which, when more active, is associated to poorer prognosis (Gopal *et al*, 2014; Fischer *et al*, 2018).

To evaluate resistance to cytotoxic treatment we chose carboplatin for its current use as the first line in chemotherapeutic management of melanomas (Pflugfelder *et al*, 2011). G10 presenting resistance to treatment supports this cell line as being enriched in slow-cycling cells, as seen in Fig. 3. It also brings one more feature to the model, for new drugs and treatments should be tested in different intratumoral phenotypes in order to achieve good results. Corroborating with this we found that the G10 cell line does not present a specific doubling time (Fig. 5), which was not the case for the other cell lines (Fig. 4). That fact that G10 cells take more time to double its population when the cell density increases (Fig. 5) is a strong indication that this cell line presents the slow-cycling phenotype. Corroborating with those findings the results of the cell cycle analysis indicate that G10 does indeed present cell cycle arrest to G0/G1 phase when compared to all other cell lines (see in Fig. 7). A similar phenomenon has been identified in a non-tumorigenic cell line, were a spontaneous slow-cycling population presented cell cycle arrest and higher p21 expression as cell density increased (Min & Spencer, 2019). The G0/G1 arrest might indicate that the cells have reversely opted out of the cell cycle, in case of a G0 stop (Zetterberg & Larsson, 1985), or are taking

longer time to follow from G1 to S phase (Williams & Stoeber, 2011). All in all the cell cycle analysis complemented the doubling times observed for A375, A7 and PCDNA3.

Once upon the findings discussed above we moved on identifying the mechanism that might be involved with the G10 cell line presenting its slow-cyling charcteristics. The slow-cycling cells not only present arrested growth but also appear to be senescent and are considered responsible for treatment resistance in many works (Cheli *et al*, 2011; Sun *et al*, 2014; Roesch *et al*, 2013). Hence, the evaluation of the SA-β-gal enzyme activity, which is more active when senescent process are taking place in the cells (Gary & Kindell, 2005). What was observed is that all cell lines of the cell panel present some level of SA-β-gal activity, however the G10 cell line presents approximately two-fold higher activity compared to all others (see in Fig. 9). With the intent of further exploring the state of activation of the senescence pathway, we searched for changes in expression of the genes involved in this pathway. P21 activity, together with p16 and p53, take part in the "senescence pathway" that ultimately suppresses the expression of genes related to cell proliferation (Collado *et al*, 2007; Narita *et al*, 2006, 2003; Yosef *et al*, 2017). As seen in Table 1, G10 presenting higher expression of the p21 gene indicates that the p53 pathway is involved in the G10 slow-cycling phenotype establishment.

Our results lead to defining the G10 cell line as a slow-cycling enriched cell line, which presents a phenotype with characteristics of senescent cells and the slow-cycling phenotype itself. If slow-cycling cells or CSCs are truly required for tumor development, growth and persistence over treatment (Roesch *et al*, 2010; Moore & Lyle, 2011; Konrad *et al*, 2016) then the aim should be to test the response of these phenotypes to novel drugs and treatments as well as Warburg-effect like phenotypes. It is clear that only by broadening the models used for treatment testing is that we will be able to fully assess tumor heterogeneity and avoid unexpected responses (Tabassum & Polyak, 2015; Gillies *et al*, 2012; McGranahan & Swanton, 2017). Concerning the senescent traits one could wonder if the G10 cell line presents a SASP phenotype (Coppé *et al*, 2010) which would match its malignant traits and its potential as a resistant phenotype and metastasis formation. Altogether, the authors hope that this cell model can be part of an effort to broaden the study objects of cancer, especially melanoma, to generate better and better ways of treatment for patients.

MATERIALS & METHODS

Cell culture

Cell lines A375, A7, G10 and PCDNA3 developed by C. Bracalente and colleagues (Bracalente *et al*, 2016b) were kindly donated by Dr. H. Durán (Consejo Nacional de Investigaciones Científicas y Tecnológicas, Buenos Aires, Argentina). Cells were mantained in 50:50 DMEM/Ham's F12 (Invitrogen®, Brazil) supplemented with 17.6 µg/ml ascorbic acid, 150 µg/ml pyruvic acid, 300 µg/ml galactose and 5 µg/ml insulin (Sigma®, Brazil). Antibiotic solution was added to the media (Sigma®, Brazil) and 10% (v/v) FBS (Gibco®, Brazil) and cells were grown at 37°C in a 5% CO_2 humidified atmosphere.

High-Resolution Respirometry (HRR) in OROBOROS Oxygraph-2K

Cellular respiration was measured at 37 °C in the two chamber respirometer Oroboros Oxygraph-2k (O2k; Oroboros Instruments, Innsbruck, Austria). Data acquisition and analysis was performed using DataLab 5 software (Oroboros Instruments, Innsbruck, Austria). Cells were trypsinized, washed with PBS and re-suspended in the same cell media as described above only lacking FBS. The final concentration in each chamber was of 0,6 x 10^5 cells in 2 mL. The protocol used consisted on oligomycin (Sigma®, Brazil), followed by several steps of carbonyl cyanide-*4*-(trifluoromethoxy)phenylhydrazone (FCCP) (Sigma®, Brazil) and rotenone (Sigma®, Brazil) with antimycin A (Sigma®, Brazil) at the end of the run (Pesta & Gnaiger, 2012).

Growth curves and doubling times

Exponentially growing cells were plated in various starting concentrations (0,5 x 10^3, 1 x 10^3, 2 x 10^3, 4 x 10^3 and 8 x 10^3) in 96-well plates and kept in culture for 2 hours (time-zero plate) and 24, 48, 72 and 96 hours. After the plates were fixed with 10% Trichloroacetic acid solution and stained with 0,5% sulforhodamine B solution. All the stained content of each well was ressuspended in 200 µL of Tris-HCl 10mM pH 10,5 solution. Absorbance was measured in 540 nm wavelength. Growth curves and doubling time were obtained with GraphPad Prism 5 software.

Cell cycle assay

Cells were trypsinized, centrifuged, washed with PBS and resuspended in 260 μL buffer (10 mM PBS, 3.5 mM trisodium citrate, 0,5 mM Tris-HCl, 0.1% v/v Igepal CA-630, 5 μg/mL

RNAse, and 2.5 μ g/mL propidium iodide/PI, pH 7.4). The cells were vortexed and incubated for 10 min on ice. The DNA content was determined by FACS Calibur (20,000 events, FL2A channel) and analyzed by FCS Express 4 software (De Novo, Canada).

Determination of senescence associated β-galactosidase activity

The C12FDG (5-Dodecanoylaminofluorescein Di-β-D-Galactopyranoside) substrate was used to measure senescence associated β-galactosidase (SA-β-gal) activity by flow cytometry. C12FDG emits green fluorescence once it is cleaved by β-galactosidase. For this assay cells were washed with PBS, harvested by trypsinization and ressuspended in a buffer containing bafilomycin (100 nM) to increase lisossome pH. After the samples are washed with PBS and stained with C12FDG (33 μM). β-galactosidase activity was estimated using the median fluorescence intensity (MFI). Samples were analyzed in Accuri C6 cytometer (BD Biosciences®) and 50,000 events were acquired through FL1 channel. Light scatter parameters were used to eliminate dead cells and subcellular debris.

p21 expression

Previous data from an Affymetrix Human Genome Chip (GeneChip® Human Gene 1.0 ST) analyzed by Bracalente and colleagues (Bracalente *et al*, 2016a) was used to determine differential expression of the p21 gene by $\log_2$ Fold Change.

Cytotoxicity assay

To assess cytotoxicity of a chemotherapeutic drug cell were plated (1 x 10^3) in 96-wells plates and treated after 24 hours. Various concentrations of carboplatin (Sigma®, Brazil) were included in the assay in order to obtain the LD50 for each cell line. After 72 hours of treatment, cells were fixed and the sulforhodamine B assay was applied the same way as mentioned above to measure cell death.

Statistical analysis

To determine each cell lines doubling time a nonlinear regression was made in order to find the exponential growth equation in Graphpad Prism 5. One-way ANOVA was used to compare doubling time means (from different starting cell densities) of the cell lines, Brown-Forsythe test was used to test variance homogeneity. To evaluate differences in response to treatment one-way ANOVA was used, followed by Tukey test. One-way ANOVA followed by Tukey

test was used for data analysis of the cell cycle assay and the β-galactosidase activity. The value $p<0.05$ was considered significant.

ACKNOWLEDGEMENTS

This study was supported by the Brazilian funds INCT-TM/CNPq/FAPESP (465458/2014-9) and MCTI/CNPQ/CBAB Cooperação Internacional em Biotecnologia (465113/2014-1). FK is recipient of fellowship awards from Conselho Nacional de Desenvolvimento Científico e Tecnológico (CNPq, Brazil). The authors would like to thank Dr. Cássio Morais Loss for the statistical consultancy.

AUTHOR CONTRIBUITIONS

CKD, IJB and FK conceived and designed the research studies; CKD, IJB, LMM, LKG collected and/or assembled the data; CKD, IJB, LMM, LKG, FCRG, FB-T, HD and FK analyzed and interpreted the data; CKD, FK and IJB wrote the manuscript. FCRG, FB-T, HD and FK provided financial support. All authors gave final approval of the manuscript.

CONFLICT OF INTEREST

The authors declare not to have any conflict of interest.

REFERENCES

Adjiri A (2017) DNA Mutations May Not Be the Cause of Cancer. *Oncol. Ther.* **5:** 85–101

Ahn A, Chatterjee A & Eccles MR (2017) The Slow Cycling Phenotype: A Growing Problem for Treatment Resistance in Melanoma. *Mol. Cancer Ther.* **16:** 1002–1009

Bettum IJ, Gorad SS, Barkovskaya A, Pettersen S, Moestue SA, Vasiliauskaite K, Tenstad E, Øyjord T, Risa Ø, Nygaard V, Mælandsmo GM & Prasmickaite L (2015) Metabolic reprogramming supports the invasive phenotype in malignant melanoma. *Cancer Lett.* **366:** 71–83

Bracalente C, Ibañez IL, Berenstein A, Notcovich C, Cerda MB, Klamt F, Chernomoretz A & Durán H (2016a) Reprogramming human A375 amelanotic melanoma cells by catalase overexpression: Upregulation of antioxidant genes correlates with regression of

melanoma malignancy and with malignant progression when downregulated. *Oncotarget* **7:** 41155–41171

Bracalente C, Rinflerch AR, Ibañez IL, García FM, Volonteri V, Galimberti GN, Klamt F & Durán H (2018) Cofilin-1 levels and intracellular localization are associated with melanoma prognosis in a cohort of patients. *Oncotarget* **9:** 24097–24108

Bracalente C, Salguero N, Notcovich C, Müller CB, da Motta LL, Klamt F, Ibañez IL & Durán H (2016b) Reprogramming human A375 amelanotic melanoma cells by catalase overexpression: Reversion or promotion of malignancy by inducing melanogenesis or metastasis. *Oncotarget* **7:** 41142–41153

Bray F, Ferlay J, Soerjomataram I, Siegel RL, Torre LA & Jemal A (2018) Global cancer statistics 2018: GLOBOCAN estimates of incidence and mortality worldwide for 36 cancers in 185 countries. *CA. Cancer J. Clin.* **68:** 394–424

Brazil. Health Ministry. Instituto Nacional do Câncer (2018) Estimativa Incidência de Câncer no Brasil - Biênio 2018-2019

Cheli Y, Guiliano S, Botton T, Rocchi S, Hofman V, Hofman P, Bahadoran P, Bertolotto C, Ballotti R & Ballotti R (2011) Mitf is the key molecular switch between mouse or human melanoma initiating cells and their differentiated progeny. *Oncogene* **30:** 2307–2318

Collado M, Blasco MA & Serrano M (2007) Cellular Senescence in Cancer and Aging. *Cell* **130:** 223–233

Coppé J-P, Desprez P-Y, Krtolica A & Campisi J (2010) The Senescence-Associated Secretory Phenotype: The Dark Side of Tumor Supression. *Annu. Rev. Pathol. Mech. Dis.* **5:** 99–118

Fischer GM, Gopal YNV, McQuade JL, Peng W, DeBerardinis RJ & Davies MA (2018) Metabolic Strategies of Melanoma Cells: Mechanisms, Interactions with the Tumor Microenvirontment, an Therapeutic Implications. *Pigment Cell Melanoma Res.* **31:** 11–30

Gary RK & Kindell SM (2005) Quantitative assay of senescence-associated β-galactosidase activity in mammalian cell extracts. *Anal. Biochem.* **343:** 329–334

Gilchrest BA, Eller MS, Geller AC & Yaar M (1999) The Pathogenesis of Melanoma Induced by Ultraviolet Radiation. *N. Engl. J. Med.* **340:** 1341–1348

Gillies RJ, Verduzco D & Gatenby RA (2012) Evolutionary dynamics of carcinogenesis and why targeted therapy does not work. *Nat. Rev. Cancer* **12:** 487–493

Gopal YN V., Rizos H, Chen G, Deng W, Frederick DT, Cooper ZA, Scolyer RA, Pupo G, Komurov K, Sehgal V, Zhang J, Patel L, Pereira CG, Broom BM, Mills GB, Ram P, Smith PD, Wargo JA, Long G V. & Davies MA (2014) Inhibition of mTORC1/2 Overcomes Resistance to MAPK Pathway Inhibitors Mediated by PGC1 and Oxidative Phosphorylation in Melanoma. *Cancer Res.* **74:** 7037–7047

Greaves M (2015) Evolutionary determinants of cancer. *Cancer Discov.* **5:** 806–20

Hall A, Meyle KD, Lange MK, Klima M, Sanderhoff M, Dahl C, Abildgaard C, Thorup K, Moghimi SM, Jensen PB, Bartek J, Guldberg P & Christensen C (2013) Dysfunctional

oxidative phosphorylation makes malignant melanoma cells addicted to glycolysis driven by the V600EBRAF oncogene. *Oncotarget* **4:** 584–599

Hamburger AW & Salmon SE (1977) Primary bioassay of human tumor stem cells. *Science* **197:** 461–3

Hanahan D & Weinberg RA (2011) Hallmarks of cancer: The next generation. *Cell* **144:** 646–674

Vander Heiden MG, Cantley LC & Thompson CB (2009) Understanding the Warburg Effect: The Metabolic Requirements of Cell Proliferation. *Science (80-.).* **324:** 1029–1033

Hoang-Minh LB, Siebzehnrubl FA, Yang C, Suzuki-Hatano S, Dajac K, Loche T, Andrews N, Schmoll Massari M, Patel J, Amin K, Vuong A, Jimenez-Pascual A, Kubilis P, Garrett TJ, Moneypenny C, Pacak CA, Huang J, Sayour EJ, Mitchell DA, Sarkisian MR, et al (2018) Infiltrative and drug-resistant slow-cycling cells support metabolic heterogeneity in glioblastoma. *EMBO J.* **37:** e98772

Konrad CV, Murali R, Varghese BA & Nair R (2016) The role of cancer stem cells in tumor heterogeneity and resistance to therapy. *Can. J. Physiol. Pharmacol.* **95:** 1–15

Leonardi GC, Falzone L, Salemi R, Zanghì A, Spandidos DA, Mccubrey JA, Candido S & Libra M (2018) Cutaneous melanoma: From pathogenesis to therapy. *Int. J. Oncol.* **52:** 1071–1080

McGranahan N & Swanton C (2015) Biological and therapeutic impact of intratumor heterogeneity in cancer evolution. *Cancer Cell* **27:** 15–26

McGranahan N & Swanton C (2017) Clonal Heterogeneity and Tumor Evolution: Past, Present, and the Future. *Cell* **168:** 613–628

Min M & Spencer SL (2019) Spontaneously slow-cycling subpopulations of human cells originate from activation of stress-response pathways. *PLOS Biol.***:** 1–25

Moore N & Lyle S (2011) Quiescent , Slow-Cycling Stem Cell Populations in Cancer : A Review of the Evidence and Discussion of Significance. **2011:**

Morrison SJ, Magee JA & Piskounova E (2012) Cancer Stem Cells: Impact, Heterogeneity, and Uncertainty. *Cancer Cell* **21:** 283–296

Narita M, Narita M, Krizhanovsky V, Nuñez S, Chicas A, Hearn SA, Myers MP & Lowe SW (2006) A Novel Role for High-Mobility Group A Proteins in Cellular Senescence and Heterochromatin Formation. *Cell* **126:** 503–514

Narita M, Nũnez S, Heard E, Narita M, Lin AW, Hearn SA, Spector DL, Hannon GJ & Lowe SW (2003) Rb-mediated heterochromatin formation and silencing of E2F target genes during cellular senescence. *Cell* **113:** 703–16

Pennello G, Devesa S & Gail M (2000) Association of surface ultraviolet B radiation levels with melanoma and nonmelanoma skin cancer in United States blacks. *Cancer Epidemiol. Biomarkers Prev.* **9:** 291–7

Perego M, Maurer M, Wang JX, Shaffer S, Müller AC, Parapatics K, Li L, Hristova D, Shin S, Keeney F, Liu S, Xu X, Raj A, Jensen JK, Bennett KL, Wagner SN, Somasundaram R

& Herlyn M (2018) A slow-cycling subpopulation of melanoma cells with highly invasive properties. *Oncogene* **37:** 302–312

Pesta D & Gnaiger E (2012) *High-Resolutin Respirometry: OXPHOS Protocols for Human Cells and Permeabilized Fibers from Small Biopsies of Human Muscle.* OROBOROS, Innsbruck, Austria.

Pflugfelder A, Eigentler TK, Keim U, Weide B, Leiter U, Ikenberg K, Berneburg M & Garbe C (2011) Effectiveness of carboplatin and paclitaxel as first- and second-line treatment in 61 patients with metastatic melanoma. *PLoS One* **6:** e16882

Ravindram Menon D, Das S, Krepler C, Vultur A, Rinner B, Schauer S, Kashofer K, Wagner K, Zhang G, Bonyadi Rad E, Haass N, Soyer H, Gabrielli B, Somasundaram R, Hoefler G, Herlyn M & Schaider H (2015) A stress-induced early innate response causes multidrug tolerance in melanoma. *Oncogene* **34:** 4448–4459

Reya T, Morrison SJ, Clarke MF & Weissman IL (2001) Stem cells, cancer, and cancer stem cells. *Nature* **414:** 105–111

Roesch A, Fukunaga-Kalabis M, Schmidt EC, Zabierowski SE, Brafford PA, Vultur A, Basu D, Gimotty P, Vogt T & Herlyn M (2010) A Temporarily Distinct Subpopulation of Slow-Cycling Melanoma Cells Is Required for Continuous Tumor Growth. *Cell* **141:** 583–594

Roesch A, Vultur A, Bogeski I, Wang H, Zimmermann KM, Speicher D, Körbel C, Laschke MW, Gimotty PA, Philipp SE, Krause E, Pätzold S, Villanueva J, Krepler C, Fukunaga-Kalabis M, Hoth M, Bastian BC, Vogt T & Herlyn M (2013) Overcoming Intrinsic Multidrug Resistance in Melanoma by Blocking the Mitochondrial. *Cancer Cell* **23:** 811–825

Shackleton M, Quintana E, Fearon ER & Morrison SJ (2009) Heterogeneity in Cancer: Cancer Stem Cells versus Clonal Evolution. *Cell* **138:** 822–829

Shain AH & Bastian BC (2016) From melanocytes to melanomas. *Nat. Rev. Cancer* **16:** 345–358

Sun C, Wang L, Huang S, Heynen GJJE, Prahallad A, Robert C, Haanen J, Blank C, Wesseling J, Willems SM, Zecchin D, Hobor S, Bajpe PK, Lieftink C, Mateus C, Vagner S, Grernrum W, Hofland I, Schlicker A, Wessels LFA, et al (2014) Reversible and adaptive resistance to BRAF(V600E) inhibition in melanoma. *Nature* **508:** 118–122

Tabassum DP & Polyak K (2015) Tumorigenesis: It takes a village. *Nat. Rev. Cancer* **15:** 473–483

Vazquez F, Lim J-H, Chim H, Bhalla K, Girnun G, Pierce K, Clish CB, Granter SR, Widlund HR, Spiegelman BM & Puigserver P (2013) PGC1α Expression Defines a Subset of Human Melanoma Tumors with Increased Mitochondrial Capacity and Resistance to Oxidative Stress. *Cancer Cell* **23:** 287–301

Verduzco D, Flaherty KT & Smalley KSM (2015) Feeling energetic? New strategies to prevent metabolic reprogramming in melanoma. *Exp. Dermatol.* **24:** 657–658

Visvader JE & Lindeman GJ (2008) Cancer stem cells in solid tumours: Accumulating evidence and unresolved questions. *Nat. Rev. Cancer* **8:** 755–768

Webster MR, Xu M, Kinzler KA, Kaur A, Appleton J, O'Connell MP, Marchbank K, Valiga A, Dang VM, Perego M, Zhang G, Slipicevic A, Frederik K, Lehrmann E, Wood III W, Becker KG, Kossenkov A V, Frederik DT, Flaherty KT, Xu X, et al (2015) Wnt5A promotes an adaptive, senescent-like stress response, while continuing to drive invasion in melanoma cells. *Pigment Cell Melanoma Res.* **28:** 184–195

Williams GH & Stoeber K (2011) The cell cycle and cancer. *J. Pathol.* **226:** 352–364

Yosef R, Pilpel N, Papismadov N, Gal H, Ovadya Y, Vadai E, Miller S, Porat Z, Ben-Dor S & Krizhanovsky V (2017) p21 maintains senescent cell viability under persistent DNA damage response by restraining JNK and caspase signaling. *EMBO J.* **36:** 2280–2295

Zetterberg A & Larsson O (1985) Kinetic analysis of regulatory events in G1 leading to proliferation or quiescence of Swiss 3T3 cells. *Proc. Natl. Acad. Sci. U. S. A.* **82:** 5365–9

FIGURE LEGENDS

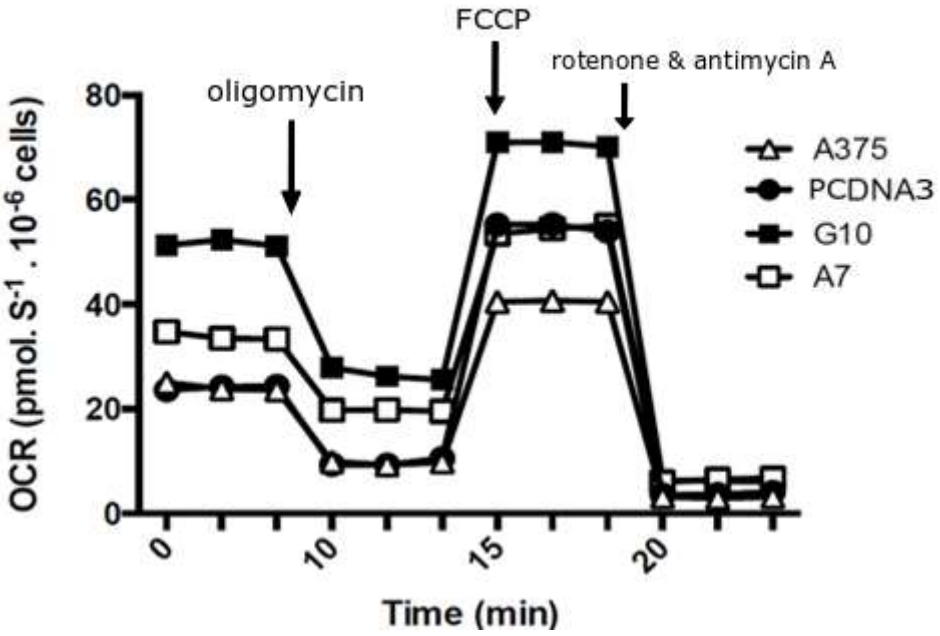

Figure 1: A375, A7, G10 and PCDNA3 respiratory profiles.

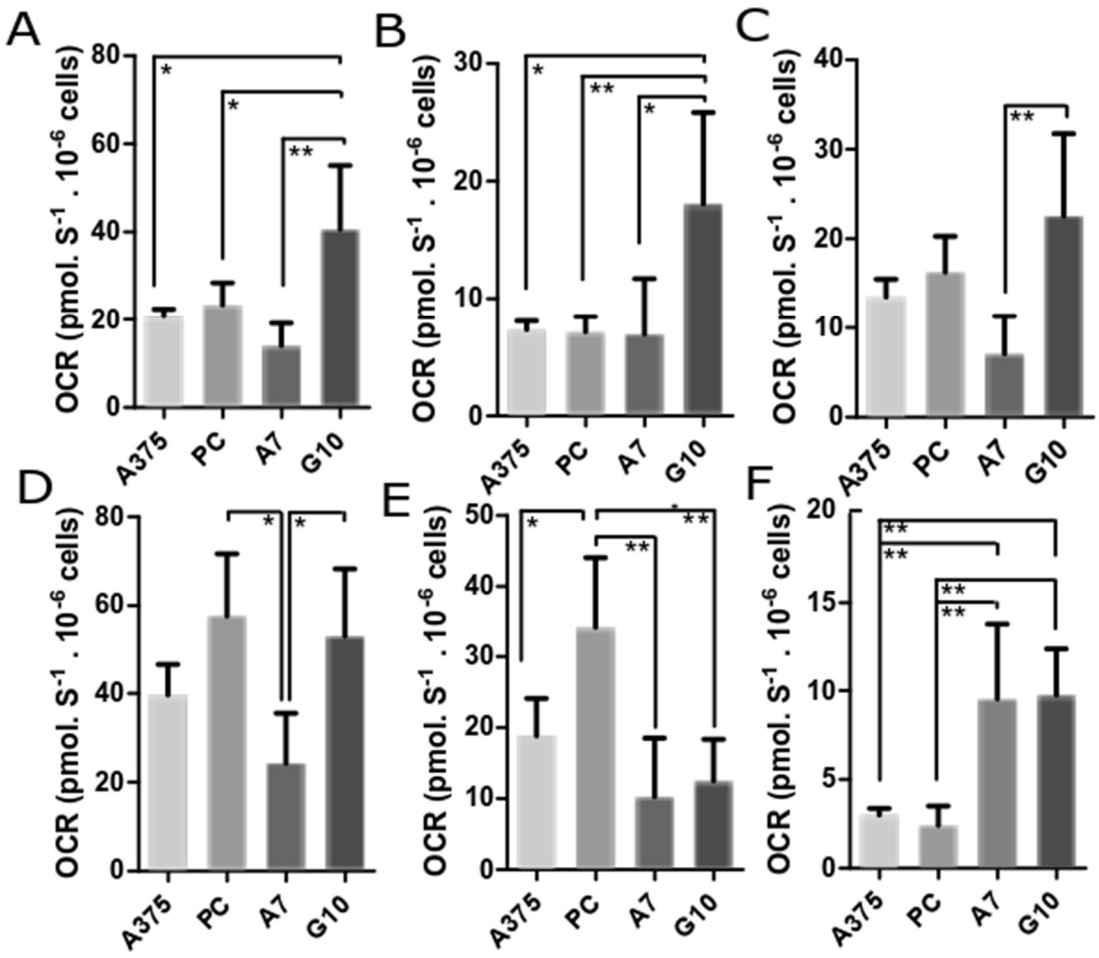

Figure 2: Aspects of A375, A7, G10 and PCDNA3 (PC) respiratory profiles.

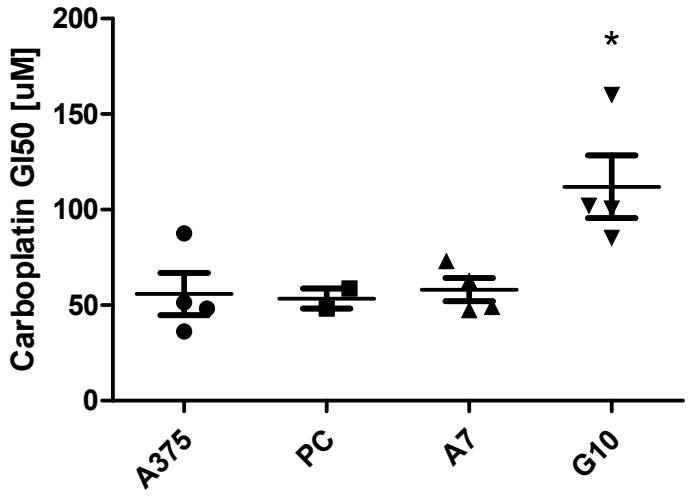

Figure 3: Comparison of the carboplatin GI50 doses for A375, PCDNA3 (PC), A7 and G10 cell lines.

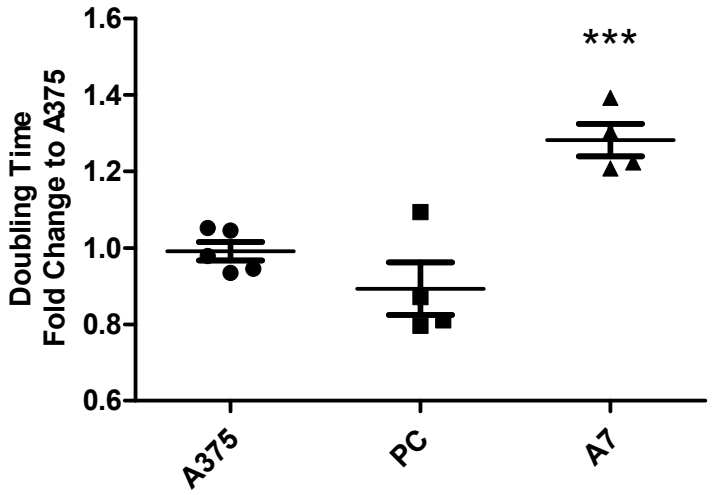

Figure 4: Doubling times of PCDNA3 (PC) and A7 compared in fold change to A375 doubling time.

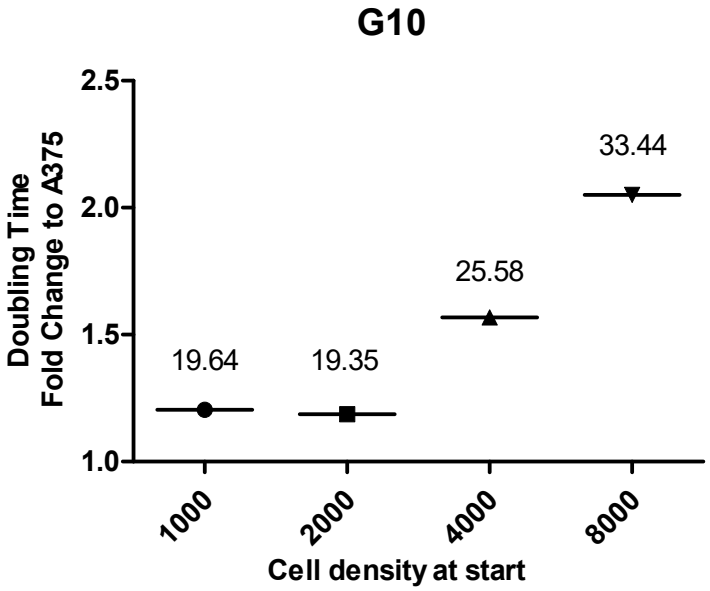

Figure 5: G10 cell line doubling times depending on cell density at start of experiment.

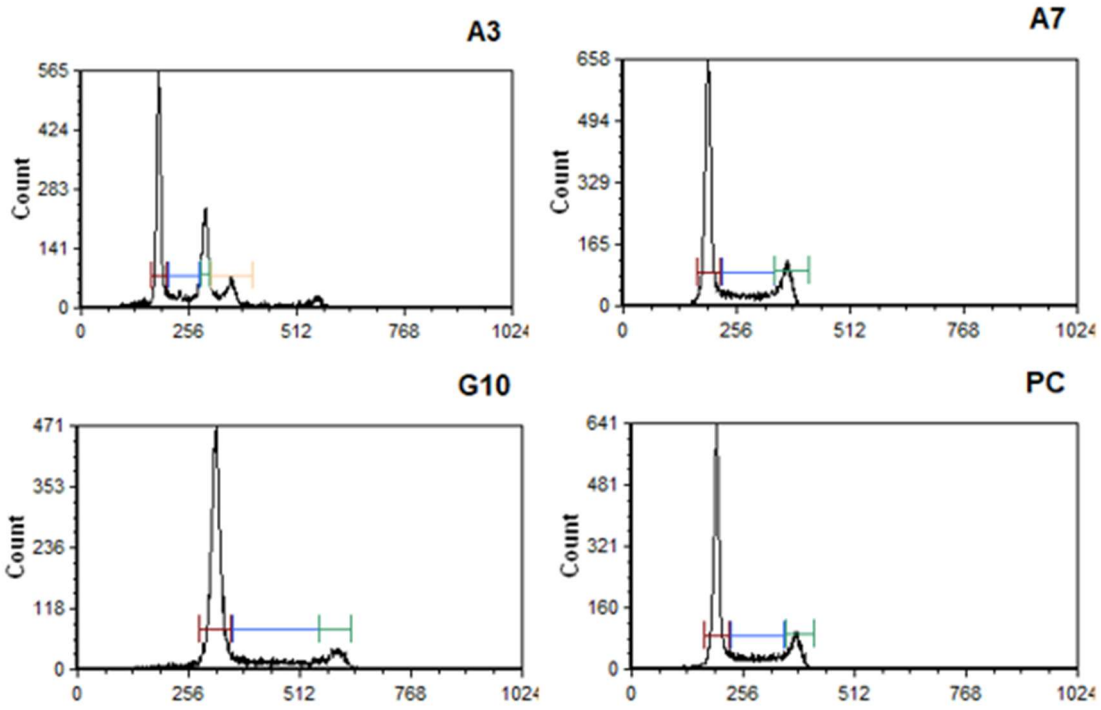

Figure 6: Cell cycle assay plots for A375 (A3), A7, G10 and PCDNA3 (PC).

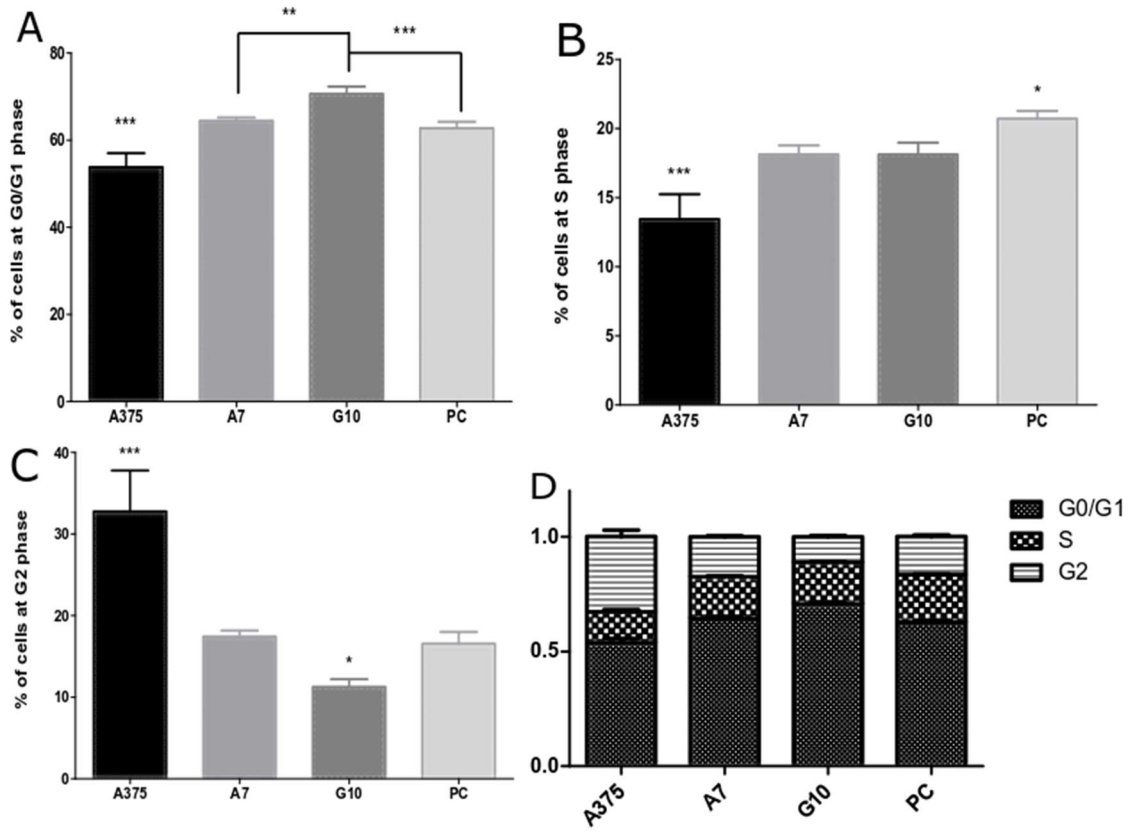

Figure 7: Cell cycle profile of each cell line: A3755, A7, G10 and PCDNA3 (PC).

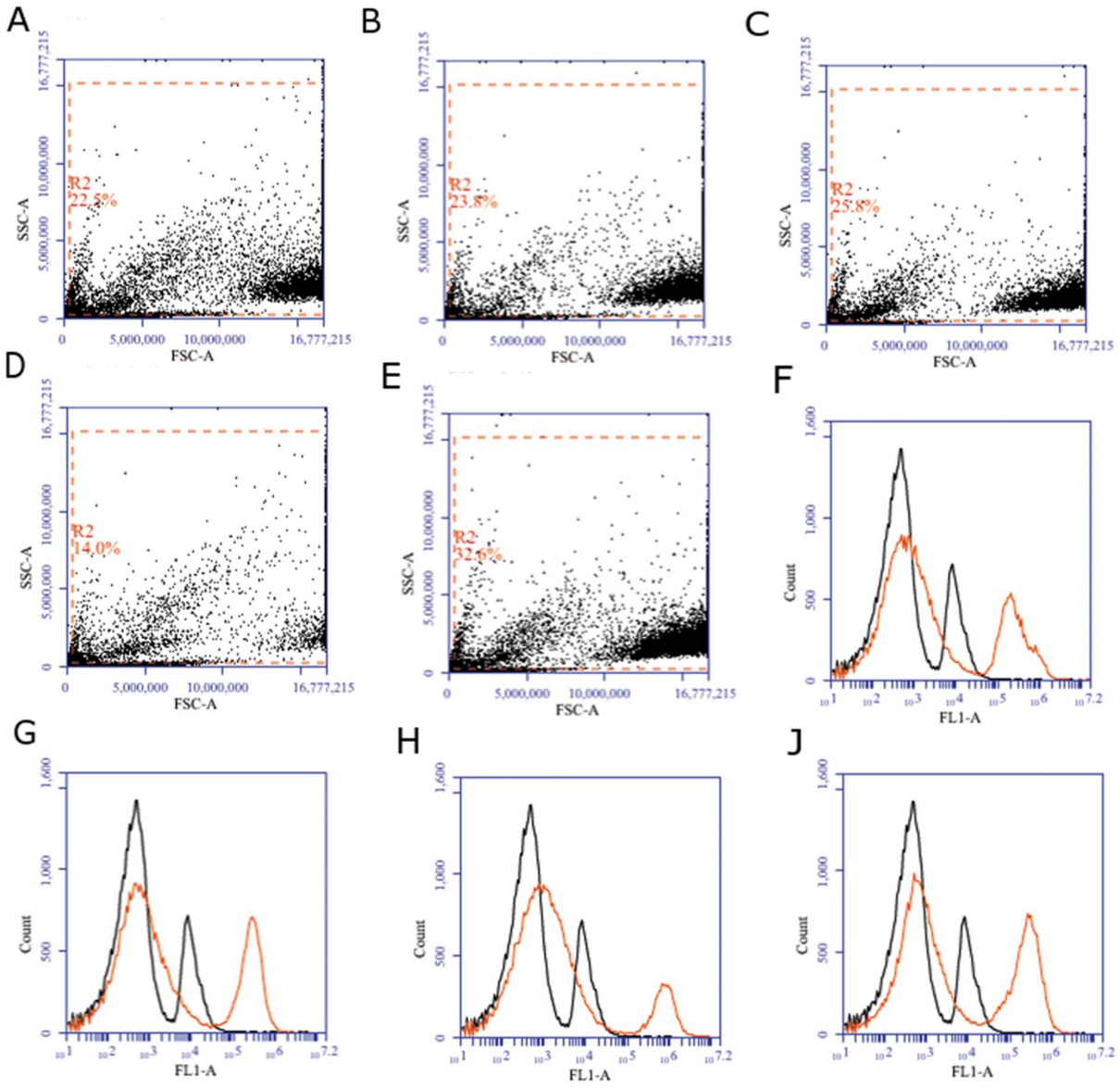

Figure 8: Dot plots and histograms of the SA-β-gal enzyme assay.

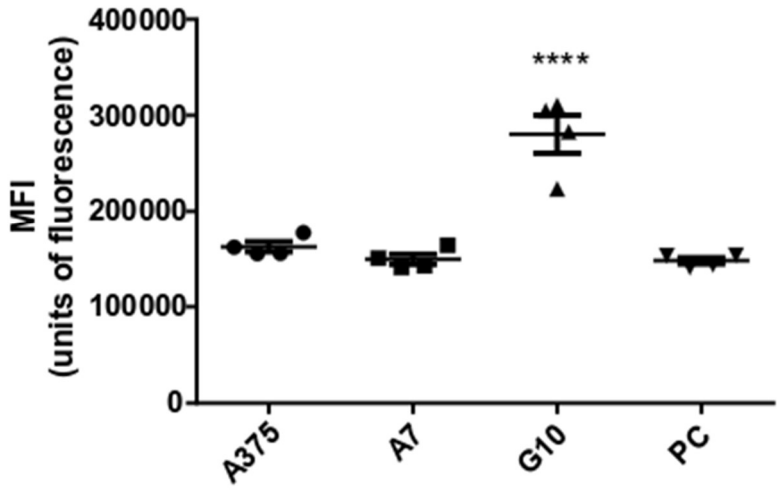

Figure 9: Mean Fluorescence Intensity (MFI) of the SA-β-gal enzyme assay for each cell line: A375, A7, G10 and PCDNA3 (PC).

EXPANDED FIGURE LEGENDS

Figure 1: A375, A7, G10 and PCDNA3 respiratory profiles. Addition of oligomycin inhibits mitochondrial respiration linked to ATP synthesis, FCCP addition allows observation of the maximum electron transfer capacity. Finally, rotenone and antimycin A block the respiratory complexes I and III, respectively.

Figure 2: Aspects of A375, A7, G10 and PCDNA3 (PC) respiratory profiles. A) Basal respiration is defined here as respiration in cell media with endogenous substrate use. B) LEAK respiration is determined by inhibition of ATP synthase with oligomycin. C) Respiration coupled to ATP synthesis is obtained subtracting leak respiration from basal respiration. D) Maximum respiration is determined by uncoupling of oxidative phosphorylation with FCCP titration. E) Reserve capacity is determined by subtraction of basal respiration from maximum respiration. F) The residual oxygen consumption (ROX) is determined by inhibition of mitochondrial respiration.

Figure 3: Comparison of the carboplatin GI50 doses for A375, PCDNA3 (PC), A7 and G10 cell lines. G10 presented higher GI50 when compared to all other cell lines.

Figure 4: Doubling times of PCDNA3 (PC) and A7 compared in fold change to A375 doubling time. A375 doubling time was 16.3 hours, PCDNA3 doubling time was 14.6 hours and A7 doubling time was 20.9 hours.

Figure 5: G10 cell line doubling times depending on cell density at start of experiment. At higher cell densities G10 was capable of modulating its proliferation rate and increased doubling time up to 1.7 fold compared to the lowest density doubling time.

Figure 6: Cell cycle assay plots for A375 (A3), A7, G10 and PCDNA3 (PC). Purple marking indicates G0/G1 phase, blue marking indicates S phase and green marking indicates G2 phase. Yellow marking indicates 4n cells.

Figure 7: Cell cycle profile of each cell line: A3755, A7, G10 and PCDNA3 (PC). A) Percent of cells on G0/G1 phases. B) Percent of cells on S phase. C) Percent of cells on G2 phase. D) Total distribution of the cell cycle phases for each cell line.

Figure 8: Dot plots and histograms of the SA-β-gal enzyme assay. Dot plots (SSC x FSC) of negative control (A) A375 (B), A7 (C), G10 (D) and PC (E). Histograms show in black the negative control and in red CD12FDG fluorescence of A375 (F), A7 (G), G10 (H) and PCDNA3 (J).

Figure 9: Means of the Mean Fluorescence Intensity (MFI) of the SA-β-gal for each cell line: A375, A7, G10 and PCDNA3 (PC). Measurements were made in arbitrary units of fluorescence. G10 cell line presented higher MFI when compared to all other cell lines.

TABLES

Pair of Comparison	Log_2 Fold Change of Expression
PCDNA3 *vs.* A375	0,1295
A7 *vs.* A375	0,4247
G10 *vs.* A375	1,0697
A7 *vs.* G10	-0,6450
A7 *vs.* PCDNA3	0,2952
G10 *vs.* PCDNA3	0,9403

Table 1: Differential expression values of p21 for each cell line comparison.

Log2 Fold Change in expression of the p21 gene the value is attributed to the first cell line in each comparison. A positive value indicates greater expression of the p21 gene on the first cell line the comparison in question, and a negative value indicates lesser expression of the p21 gene.

3 CONCLUSÕES E PERSPECTIVAS

Neste trabalho exploramos a bioenergética e estado no ciclo celular de um painel de linhagens celulares, derivadas da linhagem A375 de melanoma amelanocítico humano, A375, A7, G10 e PCDNA3 (controle de transfecção). Estas linhagens apresentam diferentes níveis de agressividade, taxas de crescimento e sensibilidade frente ao tratamento com carboplatina. O painel de células composto por estas linhagens pode ser utilizado no estudo de novas terapias contra o melanoma de forma mais abrangente do que outros modelos. A heterogeneidade tumoral deve ser um tema considerado como prioridade nos estudos do melanoma, assim como em todos outros tipos de câncer. Dessa forma propomos o uso deste painel de células como um auxílio neste quesito de inclusão da heterogeneidade tumoral em estudos de novas drogas contra o melanoma, por exemplo.

Além disso, destacamos a linhagem G10 como uma linhagem celular enriquecida em células do fenótipo de ciclagem lenta e/ou célula tronco tumoral. Em todos os experimentos realizados esta linhagem apresentou características distintas. Dentre estas destacamos a mudança na taxa de replicação mediante diferente densidade inicial de cultivo. Este fato combinado com o metabolismo altamente oxidativo apresentado por esta linhagem celular levou os autores a buscarem pelos mecanismos subjacentes a este fenômeno de ciclagem lenta. Ainda corroborando com os resultados anteriores a linhagem G10 apresentou resistência ao quimioterápico carboplatina, outra característica do fenótipo de ciclagem lenta. Também foi observado que a linhagem G10 apresenta maior quantidade de células nas fases G0 e G1 do ciclo celular, corroborando com outros resultados. O arraste no ciclo celular, por sua vez, pode ser explicado por uma maior atividade da β-galactosidase associada a senescência, observado na linhagem G10 em relação às outras linhagens do painel.

Este trabalho apresenta uma linhagem enriquecida em células de ciclagem lenta, algo original na literatura científica, dentro de um painel heterogêneo de células de melanoma humano.

Como perspectivas pretendemos avaliar a expressão do gene *JARID1B*, marcador de células de ciclagem lenta. Além disso também pretendemos avaliar a morfologia e funcionamento das mitocôndrias de cada linhagem de forma a complementar os resultados da bioenergética celular apresentados aqui.

REFERÊNCIAS

ABBAS, Tarek; DUTTA, Anindya. p21 in cancer: intricate networks and multiple activities. **Nature Reviews Cancer**, [s. l.], v. 9, n. 6, p. 400–414, 2009. Disponível em: <http://www.ncbi.nlm.nih.gov/pubmed/19440234>. Acesso em: 20 jun. 2019.

ABILDGAARD, Cecilie; GULDBERG, Per. Molecular drivers of cellular metabolic reprogramming in melanoma. **Trends in Molecular Medicine**, [s. l.], v. 21, n. 3, p. 164–171, 2015. Disponível em: <http://dx.doi.org/10.1016/j.molmed.2014.12.007>

ADJIRI, Adouda. DNA Mutations May Not Be the Cause of Cancer. **Oncology and therapy**, [s. l.], v. 5, n. 1, p. 85–101, 2017. Disponível em: <http://www.ncbi.nlm.nih.gov/pubmed/28680959>. Acesso em: 8 jun. 2019.

AHN, Antonio; CHATTERJEE, Aniruddha; ECCLES, Michael R. The Slow Cycling Phenotype: A Growing Problem for Treatment Resistance in Melanoma. **Molecular Cancer Therapeutics**, [s. l.], v. 16, n. 6, p. 1002–1009, 2017. a. Disponível em: <http://mct.aacrjournals.org/lookup/doi/10.1158/1535-7163.MCT-16-0535>

AHN, Antonio; CHATTERJEE, Aniruddha; ECCLES, Michael R. The Slow Cycling Phenotype: A Growing Problem for Treatment Resistance in Melanoma. **Molecular Cancer Therapeutics**, [s. l.], v. 16, n. 6, p. 1002–1009, 2017. b. Disponível em: <http://mct.aacrjournals.org/lookup/doi/10.1158/1535-7163.MCT-16-0535>

BETTUM, Ingrid J. et al. Metabolic reprogramming supports the invasive phenotype in malignant melanoma. **Cancer Letters**, [s. l.], v. 366, n. 1, p. 71–83, 2015. Disponível em: <http://dx.doi.org/10.1016/j.canlet.2015.06.006>

BLAGOSKLONNY, Mikhail V. Why Therapeutic Response May Not Prolong the Life of a Cancer Patient: Selection for Oncogenic Resistance. **Cell Cycle**, [s. l.], v. 4, n. 12, p. 1693–1698, 2005. Disponível em: <https://www.tandfonline.com/doi/full/10.4161/cc.4.12.2259>. Acesso em: 4 jun. 2019.

BRACALENTE, Candelaria et al. Reprogramming human A375 amelanotic melanoma cells by catalase overexpression: Upregulation of antioxidant genes correlates with regression of melanoma malignancy and with malignant progression when downregulated. **Oncotarget**, [s. l.], v. 7, n. 27, p. 41155–41171, 2016. a. Disponível em: <http://www.ncbi.nlm.nih.gov/pubmed/27206673>

BRACALENTE, Candelaria et al. Reprogramming human A375 amelanotic melanoma cells by catalase overexpression: Reversion or promotion of malignancy by inducing melanogenesis or metastasis. **Oncotarget**, [s. l.], v. 7, n. 27, p. 41142–41153, 2016. b. Disponível em: <http://www.oncotarget.com/abstract/9220%0Ahttp://www.ncbi.nlm.nih.gov/pubmed/27206672%0Ahttp://www.pubmedcentral.nih.gov/articlerender.fcgi?artid=PMC5173048>

BRACALENTE, Candelaria et al. Cofilin-1 levels and intracellular localization are associated with melanoma prognosis in a cohort of patients. **Oncotarget**, [s. l.], v. 9, n. 35, p. 24097–24108, 2018.

BRAY, Freddie et al. Global cancer statistics 2018: GLOBOCAN estimates of incidence and

mortality worldwide for 36 cancers in 185 countries. **CA: a cancer journal for clinicians**, [s. l.], v. 68, n. 6, p. 394–424, 2018. Disponível em: <http://www.ncbi.nlm.nih.gov/pubmed/30207593>

CAZZALINI, Ornella et al. Multiple roles of the cell cycle inhibitor p21CDKN1A in the DNA damage response. **Mutation Research/Reviews in Mutation Research**, [s. l.], v. 704, n. 1–3, p. 12–20, 2010. Disponível em: <http://www.ncbi.nlm.nih.gov/pubmed/20096807>. Acesso em: 20 jun. 2019.

CHAPMAN, Paul B. et al. Improved Survival with Vemurafenib in Melanoma with BRAF V600E Mutation. **The New England Journal of Medicine**, [s. l.], v. 364, n. 26, p. 2507–2516, 2011. Disponível em: <http://www.nejm.org/doi/abs/10.1056/NEJMoa1103782>

CHELI, Y. et al. Mitf is the key molecular switch between mouse or human melanoma initiating cells and their differentiated progeny. **Oncogene**, [s. l.], v. 30, n. 20, p. 2307–2318, 2011. Disponível em: <http://www.ncbi.nlm.nih.gov/pubmed/21278797>. Acesso em: 14 jun. 2019.

COLLADO, Manuel; BLASCO, Maria A.; SERRANO, Manuel. Cellular Senescence in Cancer and Aging. **Cell**, [s. l.], v. 130, n. 2, p. 223–233, 2007. Disponível em: <http://www.ncbi.nlm.nih.gov/pubmed/17662938>. Acesso em: 15 jun. 2019.

COPPÉ, Jean-Philippe et al. The Senescence-Associated Secretory Phenotype: The Dark Side of Tumor Suppression. **Annual Review of Pathology: Mechanisms of Disease**, [s. l.], v. 5, n. 1, p. 99–118, 2010. b. Disponível em: <http://www.ncbi.nlm.nih.gov/pubmed/20078217>. Acesso em: 4 jun. 2019.

DEY, B. K. et al. The Histone Demethylase KDM5b/JARID1b Plays a Role in Cell Fate Decisions by Blocking Terminal Differentiation. **Molecular and Cellular Biology**, [s. l.], v. 28, n. 17, p. 5312–5327, 2008. Disponível em: <http://mcb.asm.org/cgi/doi/10.1128/MCB.00128-08>

EWALD, Jonathan A. et al. Therapy-induced senescence in cancer. **Journal of the National Cancer Institute**, [s. l.], v. 102, n. 20, p. 1536–46, 2010. Disponível em: <http://www.ncbi.nlm.nih.gov/pubmed/20858887>. Acesso em: 20 jun. 2019.

FISCHER, Grant M. et al. Metabolic Strategies of Melanoma Cells: Mechanisms, Interactions with the Tumor Microenvirontment, an Therapeutic Implications. **Pigment Cell and Melanoma Research**, [s. l.], v. 31, n. 1, p. 11–30, 2018.

GARY, Ronald K.; KINDELL, Susan M. Quantitative assay of senescence-associated β-galactosidase activity in mammalian cell extracts. **Analytical Biochemistry**, [s. l.], v. 343, n. 2, p. 329–334, 2005.

GATENBY, R. A.; CUNNINGHAM, J. J.; BROWN, J. S. Evolutionary triage governs fitness in driver and passenger mutations and suggests targeting never mutations. **Nature Communications**, [s. l.], v. 5, n. 1, p. 5499, 2014. Disponível em: <http://www.nature.com/articles/ncomms6499>. Acesso em: 28 maio. 2019.

GEWIRTZ, D. A. A critical evaluation of the mechanisms of action proposed for the antitumor effects of the anthracycline antibiotics adriamycin and daunorubicin. **Biochemical pharmacology**, [s. l.], v. 57, n. 7, p. 727–41, 1999. Disponível em:

<http://www.ncbi.nlm.nih.gov/pubmed/10075079>. Acesso em: 20 jun. 2019.

GILCHREST, Barbara A. et al. The Pathogenesis of Melanoma Induced by Ultraviolet Radiation. **New England Journal of Medicine**, [s. l.], v. 340, n. 17, p. 1341–1348, 1999. Disponível em: <http://www.ncbi.nlm.nih.gov/pubmed/10219070>. Acesso em: 19 nov. 2018.

GILLIES, Robert J.; VERDUZCO, Daniel; GATENBY, Robert A. Evolutionary dynamics of carcinogenesis and why targeted therapy does not work. **Nature Reviews Cancer**, [s. l.], v. 12, n. 7, p. 487–493, 2012. Disponível em: <http://dx.doi.org/10.1038/nrc3298>

GOPAL, Y. N. V. et al. Inhibition of mTORC1/2 Overcomes Resistance to MAPK Pathway Inhibitors Mediated by PGC1 and Oxidative Phosphorylation in Melanoma. **Cancer Research**, [s. l.], v. 74, n. 23, p. 7037–7047, 2014. Disponível em: <http://www.ncbi.nlm.nih.gov/pubmed/25297634>. Acesso em: 4 jun. 2019.

GREAVES, Mel. Evolutionary determinants of cancer. **Cancer discovery**, [s. l.], v. 5, n. 8, p. 806–20, 2015. Disponível em: <http://www.ncbi.nlm.nih.gov/pubmed/26193902>. Acesso em: 14 jun. 2019.

HALL, Arnaldur et al. Dysfunctional oxidative phosphorylation makes malignant melanoma cells addicted to glycolysis driven by the V600EBRAF oncogene. **Oncotarget**, [s. l.], v. 4, n. 4, p. 584–599, 2013.

HAMBURGER, A. W.; SALMON, S. E. Primary bioassay of human tumor stem cells. **Science**, [s. l.], v. 197, n. 4302, p. 461–3, 1977. Disponível em: <http://www.ncbi.nlm.nih.gov/pubmed/560061>. Acesso em: 10 jun. 2019.

HANAHAN, Douglas; WEINBERG, Robert A. Hallmarks of cancer: The next generation. **Cell**, [s. l.], v. 144, n. 5, p. 646–674, 2011. Disponível em: <http://dx.doi.org/10.1016/j.cell.2011.02.013>

HAQ, Rizwan et al. Oncogenic BRAF Regulates Oxidative Metabolism via PGC1α and MITF. **Cancer Cell**, [s. l.], v. 23, n. 3, p. 302–315, 2013. Disponível em: <http://www.ncbi.nlm.nih.gov/pubmed/23477830>. Acesso em: 20 jun. 2019.

HEPPNER, G. H. Tumor heterogeneity. **Cancer research**, [s. l.], v. 44, n. 6, p. 2259–65, 1984. Disponível em: <http://www.ncbi.nlm.nih.gov/pubmed/6372991>. Acesso em: 28 maio. 2019.

HOANG-MINH, Lan B. et al. Infiltrative and drug-resistant slow-cycling cells support metabolic heterogeneity in glioblastoma. **The EMBO Journal**, [s. l.], v. 37, n. 23, p. e98772, 2018.

HODI, F. Stephen et al. Improved Survival with Ipilimumabin Patients with Metastatic Melanoma. **The New England Journal of Medicine**, [s. l.], v. 363, n. 8, p. 771–723, 2010.

HSU, Chien-Hsiang; ALTSCHULER, Steven J.; WU, Lani F. Patterns of Early p21 Dynamics Determine Proliferation-Senescence Cell Fate after Chemotherapy. **Cell**, [s. l.], p. 1–13, 2019. Disponível em: <https://linkinghub.elsevier.com/retrieve/pii/S0092867419306129>

INSTITUTO NACIONAL DO CÂNCER. Estimativa Incidência de Câncer no Brasil - Biênio

2018-2019. [s.l: s.n.]. v. 1

KONRAD, Christina Valbirk et al. The role of cancer stem cells in tumor heterogeneity and resistance to therapy. **Canadian Journal of Physiology and Pharmacology**, [s. l.], v. 95, n. 1, p. 1–15, 2016.

KUILMAN, Thomas et al. The essence of senescence. **Genes & Development**, [s. l.], v. 24, n. 22, p. 2463, 2010. Disponível em: <http://www.ncbi.nlm.nih.gov/pubmed/21078816>. Acesso em: 4 jun. 2019.

LEE, Soyoung; SCHMITT, Clemens A. The dynamic nature of senescence in cancer. **Nature Cell Biology**, [s. l.], v. 21, n. 1, p. 94–101, 2019.

LEONARDI, Giulia C. et al. Cutaneous melanoma: From pathogenesis to therapy. **International Journal of Oncology**, [s. l.], v. 52, n. 4, p. 1071–1080, 2018.

MCGRANAHAN, Nicholas; SWANTON, Charles. Biological and therapeutic impact of intratumor heterogeneity in cancer evolution. **Cancer Cell**, [s. l.], v. 27, n. 1, p. 15–26, 2015. a. Disponível em: <http://dx.doi.org/10.1016/j.ccell.2014.12.001>

MCGRANAHAN, Nicholas; SWANTON, Charles. Biological and Therapeutic Impact of Intratumor Heterogeneity in Cancer Evolution. **Cancer Cell**, [s. l.], v. 27, n. 1, p. 15–26, 2015. b. Disponível em: <http://www.ncbi.nlm.nih.gov/pubmed/25584892>. Acesso em: 28 maio. 2019.

MCGRANAHAN, Nicholas; SWANTON, Charles. Clonal Heterogeneity and Tumor Evolution: Past, Present, and the Future. **Cell**, [s. l.], v. 168, n. 4, p. 613–628, 2017. Disponível em: <http://dx.doi.org/10.1016/j.cell.2017.01.018>

MIN, Mingwei; SPENCER, Sabrina L. Spontaneously slow-cycling subpopulations of human cells originate from activation of stress-response pathways. **PLOS Biology**, [s. l.], p. 1–25, 2019.

MOORE, Nathan; LYLE, Stephen. Quiescent , Slow-Cycling Stem Cell Populations in Cancer : A Review of the Evidence and Discussion of Significance. [s. l.], v. 2011, 2011.

MORRISON, Sean J.; MAGEE, Jeffrey A.; PISKOUNOVA, Elena. Cancer Stem Cells: Impact, Heterogeneity, and Uncertainty. **Cancer Cell**, [s. l.], v. 21, n. 3, p. 283–296, 2012.

NARITA, Masashi et al. Rb-mediated heterochromatin formation and silencing of E2F target genes during cellular senescence. **Cell**, [s. l.], v. 113, n. 6, p. 703–16, 2003. Disponível em: <http://www.ncbi.nlm.nih.gov/pubmed/12809602>. Acesso em: 15 jun. 2019.

NARITA, Masashi et al. A Novel Role for High-Mobility Group A Proteins in Cellular Senescence and Heterochromatin Formation. **Cell**, [s. l.], v. 126, n. 3, p. 503–514, 2006. Disponível em: <http://www.ncbi.nlm.nih.gov/pubmed/16901784>. Acesso em: 15 jun. 2019.

NELSON, David L.; COX, Michael M. Lehningher Principles of Biochemistry. 5a edição ed. [s.l.] : W. H. Freeman and Company, 2008.

NOWELL, P. C. The clonal evolution of tumor cell populations. **Science,** [s. l.], v. 194, n. 4260, p. 23–8, 1976. Disponível em: <http://www.ncbi.nlm.nih.gov/pubmed/959840>. Acesso

em: 28 maio. 2019.

PARMENTER, Tiffany J. et al. Response of BRAF mutant melanoma to BRAF inhibition is mediated by a network of transcriptional regulators of glycolysis. **Cancer Discovery**, [s. l.], v. 4, n. 4, p. 423–433, 2014.

PENNELLO, G.; DEVESA, S.; GAIL, M. Association of surface ultraviolet B radiation levels with melanoma and nonmelanoma skin cancer in United States blacks. **Cancer epidemiology, biomarkers & prevention** : a publication of the American Association for Cancer Research, cosponsored by the American Society of Preventive Oncology, [s. l.], v. 9, n. 3, p. 291–7, 2000. Disponível em: <http://www.ncbi.nlm.nih.gov/pubmed/10750668>. Acesso em: 19 nov. 2018.

PEREGO, M. et al. A slow-cycling subpopulation of melanoma cells with highly invasive properties. **Oncogene**, [s. l.], v. 37, n. 3, p. 302–312, 2018.

PESTA, Dominik; GNAIGER, Erich. High-Resolutin Respirometry: OXPHOS Protocols for Human Cells and Permeabilized Fibers from Small Biopsies of Human Muscle. [s.l: s.n.]. v. 810 Disponível em: <http://www.springerlink.com/index/10.1007/978-1-61779-382-0>

PFLUGFELDER, Annette et al. Effectiveness of carboplatin and paclitaxel as first- and second-line treatment in 61 patients with metastatic melanoma. **PloS one**, [s. l.], v. 6, n. 2, p. e16882, 2011. Disponível em: <http://www.ncbi.nlm.nih.gov/pubmed/21359173%0Ahttp://www.pubmedcentral.nih.gov/articlerender.fcgi?artid=PMC3040212>

PINHEIRO, Céline et al. The metabolic microenvironment of melanomas: Prognostic value of MCT1 and MCT4. **Cell Cycle**, [s. l.], v. 15, n. 11, p. 1462–1470, 2016. Disponível em: <http://dx.doi.org/10.1080/15384101.2016.1175258>

RAVINDRAM MENON, D. et al. A stress-induced early innate response causes multidrug tolerance in melanoma. **Oncogene**, [s. l.], v. 34, n. 34, p. 4448–4459, 2015.

REYA, Tannishtha et al. Stem cells, cancer, and cancer stem cells. **Nature**, [s. l.], v. 414, n. 6859, p. 105–111, 2001. Disponível em: <http://www.nature.com/articles/35102167>. Acesso em: 4 jun. 2019.

ROESCH, Alexander et al. A Temporarily Distinct Subpopulation of Slow-Cycling Melanoma Cells Is Required for Continuous Tumor Growth. **Cell**, [s. l.], v. 141, n. 4, p. 583–594, 2010.

ROESCH, Alexander et al. Overcoming Intrinsic Multidrug Resistance in Melanoma by Blocking the Mitochondrial. **Cancer Cell**, [s. l.], v. 23, p. 811–825, 2013.

SAÚDE, Ministério Da. Plano Nacional de Saúde PNS 2016-2019. Brasília DF, [s. l.], 2016.

SCOTT, David A. et al. Comparative metabolic flux profiling of melanoma cell lines: Beyond the Warburg effect. **Journal of Biological Chemistry**, [s. l.], v. 286, n. 49, p. 42626–42634, 2011.

SHACKLETON, Mark et al. Heterogeneity in Cancer: Cancer Stem Cells versus Clonal Evolution. **Cell**, [s. l.], v. 138, n. 5, p. 822–829, 2009.

SHAIN, A. Hunter; BASTIAN, Boris C. From melanocytes to melanomas. **Nature Reviews Cancer**, [s. l.], v. 16, n. 6, p. 345–358, 2016. Disponível em: <http://dx.doi.org/10.1038/nrc.2016.37>

SHAY, J. W. Role of Telomeres and Telomerase in Aging and Cancer. **Cancer Discovery**, [s. l.], v. 6, n. 6, p. 584–593, 2016. Disponível em: <http://www.ncbi.nlm.nih.gov/pubmed/27029895>. Acesso em: 4 jun. 2019.

SHIMOBAYASHI, Mitsugu; HALL, Michael N. Making new contacts: the mTOR network in metabolism and signalling crosstalk. **Nature Reviews Molecular Cell Biology**, [s. l.], v. 15, n. 3, p. 155–162, 2014. Disponível em: <http://www.ncbi.nlm.nih.gov/pubmed/24556838>. Acesso em: 20 jun. 2019.

SIEGEL, Rebecca L.; MILLER, Kimberly D.; JEMAL, Ahmedin. Cancer statistics, 2017. **CA: a cancer journal for clinicians**, [s. l.], v. 67, p. 7–30, 2017. Disponível em: <http://www.ncbi.nlm.nih.gov/pubmed/30620402>

SUN, Chong et al. Reversible and adaptive resistance to BRAF(V600E) inhibition in melanoma. **Nature**, [s. l.], v. 508, n. 1, p. 118–122, 2014.

TABASSUM, Doris P.; POLYAK, Kornelia. Tumorigenesis: It takes a village. **Nature Reviews Cancer**, [s. l.], v. 15, n. 8, p. 473–483, 2015. Disponível em: <http://dx.doi.org/10.1038/nrc3971>

VANDER HEIDEN, Matthew G.; CANTLEY, Lewis C.; THOMPSON, Craig B. Understanding the Warburg Effect: The Metabolic Requirements of Cell Proliferation. **Science**, [s. l.], v. 324, p. 1029–1033, 2009.

VAZQUEZ, Francisca et al. PGC1α Expression Defines a Subset of Human Melanoma Tumors with Increased Mitochondrial Capacity and Resistance to Oxidative Stress. **Cancer Cell**, [s. l.], v. 23, n. 3, p. 287–301, 2013. Disponível em: <http://www.ncbi.nlm.nih.gov/pubmed/23416000>. Acesso em: 4 jun. 2019.

VERDUZCO, Daniel; FLAHERTY, Keith T.; SMALLEY, Keiran S. M. Feeling energetic? New strategies to prevent metabolic reprogramming in melanoma. **Experimental Dermatology**, [s. l.], v. 24, n. 9, p. 657–658, 2015.

VISVADER, Jane E.; LINDEMAN, Geoffrey J. Cancer stem cells in solid tumours: Accumulating evidence and unresolved questions. **Nature Reviews Cancer**, [s. l.], v. 8, n. 10, p. 755–768, 2008.

WARBURG, Otto. On the Origin of Cancer Cells. **Science**, [s. l.], v. 123, n. 3191, p. 309 LP – 314, 1956. Disponível em: <http://science.sciencemag.org/content/123/3191/309.abstract>

WEBSTER, Marie R. et al. Wnt5A promotes an adaptive, senescent-like stress response, while continuing to drive invasion in melanoma cells. **Pigment Cell Melanoma Res.**, [s. l.], v. 28, n. 2, p. 184–195, 2015.

WILLIAMS, Gareth H.; STOEBER, Kai. The cell cycle and cancer. **Journal of Pathology**, [s. l.], v. 226, p. 352–364, 2011.

YOSEF, Reut et al. p21 maintains senescent cell viability under persistent DNA damage

response by restraining JNK and caspase signaling. **The EMBO Journal**, [s. l.], v. 36, n. 15, p. 2280–2295, 2017.

ZETTERBERG, A.; LARSSON, O. Kinetic analysis of regulatory events in G1 leading to proliferation or quiescence of Swiss 3T3 cells. **Proceedings of the National Academy of Sciences of the United States of America**, [s. l.], v. 82, n. 16, p. 5365–9, 1985. Disponível em: <http://www.ncbi.nlm.nih.gov/pubmed/3860868>. Acesso em: 15 jun. 2019.

ZHANG, Gao et al. Targeting mitochondrial biogenesis to overcome drug resistance to MAPK inhibitors. **Journal of Clinical Investigation**, [s. l.], v. 126, n. 5, p. 1834–1856, 2016. Disponível em: <http://www.ncbi.nlm.nih.gov/pubmed/27043285>. Acesso em: 20 jun. 2019.

ANEXO A – NORMAS DE PUBLICAÇÃO DA REVISTA EMBO JOURNAL

Retirado de: http://emboj.embopress.org/authorguide#researcharticleguide

Research Article Guidelines EMBO Journal

MANUSCRIPT PREPARATION

Research Article Submission

YOU DO NOT NEED TO REFORMAT YOUR MANUSCRIPT FOR A FIRST SUBMISSION

The following guidelines refer to Research Articles. While published manuscripts are expected to conform tightly to the following guidelines, this is not a requirement at first submission.

Manuscripts must be written in clear and concise English and be intelligible to a broad readership. Prior to submission, authors may benefit from having their manuscript reviewed for clarity by colleagues and/or by using one of the many English language-editing services that are available.

Text Format

The Editorial Office will only accept text files in RTF or MS Word format. The final character count must be clearly indicated on the title page of the manuscript. Revised manuscripts that do not comply with the formatting guidelines, or exceed the length restrictions, may be returned to the authors for amendment.

Please submit the full text (including figure legends, expanded view figure legends, tables (note: tables may also be be provided as separate Word or Excel files, they need to be editable), and references) as a single MS Word or RTF file.

Submitted manuscripts should be divided into the following sections:

- Title page
- Abstract
- Introduction
- Results
- Discussion
- Materials and Methods
- Acknowledgements
- Author contributions
- Conflict of interest
- References
- Figure legends
- Tables and their legends

- Expanded View Figure legends

Title Page

The title should be short and informative, and should not contain any abbreviations (for example, Epithelial-Mesenchymal Transition should not be abbreviated to EMT). However, commonly used gene or protein acronyms are acceptable. The total length of the title should not exceed 100 characters (including spaces). Serial titles are not accepted.

The full name (middle names as initials) of each author should be given. Multiple first-authorships are acceptable and should be indicated. Numbers in superscript should be used to indicate the department, institution, city with postal code and country, for each author. Any changes of address may also be given in numbered footnotes. It is possible to name more than one author as the correspondent of a published article, although we will by default address all correspondence to the single author listed as Corresponding Author upon submission.

Please provide a running title of no more than 40 characters including spaces.

Up to five keywords, which may or may not appear in the title, should be given in alphabetical order, below the abstract, each separated by a slash (/).

Abstract

This should be a single paragraph not exceeding 175 words. The Abstract should be comprehensible to readers before they have read the paper, and abbreviations should be avoided where possible (as for the title). Reference citations within the abstract are not permitted. The abstract should describe all key novel findings of the study.

Introduction

The Introduction should be succinct and without subheadings. It should provide only the necessary background information, rather than comprise a comprehensive review of the field. Citation of the primary literature is required where appropriate (see section on Citation Policy).

Results

The Results section, and associated figures, tables and Expanded View information, must accurately describe the findings of the study. Figure, Table, Expanded View figure, Expanded View table, Expanded View movie, etc. order should follow the text. Detailed methodological descriptions should be restricted to the Materials and Methods section. ‘Data not shown’ is not permitted (see below): all significant data should be displayed in the main figures or Expanded View information.

Discussion

The Discussion should accurately interpret the results, but not be repetitive with the Results section. Authors are encouraged to discuss their work in the broader context. Related

published data must be appropriately discussed and cited. Speculation is allowed but should be clearly labelled as such. For shorter articles, the Results and Discussion sections can be combined.

Materials and Methods

This section should contain sufficient detail so that all experimental procedures can be repeated by others, in conjunction with cited references. Reagents must be described in such a way as to allow readers to identify them unequivocally and/or reproduce them. For example, antibodies epitopes should be described and siRNA and other probe sequences must be provided. In cases where detailed methods cannot be described within the length limits of the article, additional Materials and Methods can be included as part of the Appendix (see Expanded View section). This additional information should, however, not be of immediate importance for the understanding of the manuscript, and it is not permissible to move the entire "Materials and Methods" section into the Appendix.

Acknowledgements

These should be placed at the end of the text and not in footnotes. Personal acknowledgements should precede those of institutions or agencies. Grant numbers are permissible. Dedications are discouraged. It is the authors responsibility to add required funder information to the acknowledgement section before proof stage. Such information can only be added to published paper in exceptional circumstances and at the editors' discretion.

Author contributions

The journal requires a statement specifying the contributions of every author. Further details on authorship can be found here.

Conflict of interest

The journal requires a statement specifying whether or not the authors have a conflict of interest (see above for details). In the case of a conflict of interest, this must be specified.

Data Availability Section

Datasets and computer code that were generated in the reported study should be listed in a structured manner in the "Data Availability" section placed after the Materials & Methods section. Each dataset should be listed under a separate bullet point that includes 1) a short description of the measurement type (eg RNA-Seq, ChIP-Seq, mass spectrometry proteomics, imaging, etc…), 2) the name of the repository (or its recommended acronym, see table below and consult fairsharing.org); 3) the DOI or accession number of the dataset; and 4) a resolvable link to the dataset, either in the form of a resolvable link from http://identifiers.org or as the full URL to the respective database record:

Data availability

The datasets and computer code produced in this study are available in the following databases:

- RNA-Seq data: Gene Expression Omnibus GSE46843 (https://www.ncbi.nlm.nih.gov/geo/query/acc.cgi?acc=GSE46843)
- Chip-Seq data: Gene Expression Omnibus GSE46748 (https://www.ncbi.nlm.nih.gov/geo/query/acc.cgi?acc=GSE46748)
- Protein interaction AP-MS data: PRIDE PXD000208 (http://www.ebi.ac.uk/pride/archive/projects/PXD000208)
- Imaging dataset: Image Data Resource https://doi.org/10.17867/10000101
- Modeling computer scripts: GitHub (https://github.com/SysBioChalmers/GECKO/releases/tag/v1.0)
- [data type]: [name of the resource] [accession number/identifier/doi] ([URL or identifiers.org/DATABASE:ACCESSION])

Supported acronyms for databases (see also fairsharing.org):

Full name	Acronym	URL
Database of Genotypes and Phenotypes	dbGAP	https://www.ncbi.nlm.nih.gov/gap
Database of single nucleotide polymorphisms	dbSNP	https://www.ncbi.nlm.nih.gov/snp
Electron Microscopy Data Bank	EMDB	https://www.ebi.ac.uk/pdbe/emdb
European Genome-phenome Archive	EGA	https://www.ebi.ac.uk/ega
European Nucleotide Archive	ENA	https://www.ebi.ac.uk/ena
Gene Expression Omnibus	GEO	https://www.ncbi.nlm.nih.gov/geo
Image Data Resource	IDR	https://idr.openmicroscopy.or/
Molecular Interaction Database	IntAct	https://www.ebi.ac.uk/intact
Protein Data Bank	PDB	http://www.wwpdb.org
Proteomics Identification database	PRIDE	https://www.ebi.ac.uk/pride
Reference Sequence Database	RefSeq	https://www.ncbi.nlm.nih.gov/refseq
Sequence Read Archive	SRA	https://www.ncbi.nlm.nih.gov/sra

References and Citations

As a matter of policy, the journal requires the citation of **primary literature** (over review articles) and, when appropriate, of **data** (see section on Data citation below). The reference list at the journal is not subject for length restriction: within reason, all relevant citations should be included. Authors are responsible for the accuracy of the references and for ensuring that the related literature is accurately and comprehensively discussed and cited. Review articles should only be cited for general background information, or the proposal of certain concepts or similar purposes. Primary research articles should preferentially be referenced to introduce the question being addressed or to support the conclusions and interpretations of the results.

Only articles that have been published or that are accepted for publication at a named publication should be cited in the reference list. Papers accepted for publication must be cited with the corresponding author's permission and should include title and all author names (or

initials if any of the authors are co-authors of the present contribution), as well as either the DOI, if available, or the term 'in press'. In the text of the manuscript, a reference should be cited by author and year of publication; no more than two authors may be cited per reference; 'et al' should be used if there are more than two authors (i.e. Smith & Jones, 2003; Smith et al, 2000). In the reference list, citations should be listed in alphabetical order and then chronologically, with the authors' surnames and initials inverted; where there are more than 20 authors on a paper, 20 will be listed, followed by 'et al.'. Publications by the same author(s) in the same year should be identified with a, b, c after the year of publication. The name of each journal should be abbreviated according to Index Medicus and italicized. References should therefore be listed as follows:

- Akhmedkhanov A, Toniolo P, Zeleniuch-Jacquotte A, Koenig KL, Shore RE (2002) Aspirin and lung cancer in women. *Br J Cancer* 87: 49-53

Book chapters and books can be cited in the following way:

- Price SR, Oubridge C, Varani G, Nagai K (1998) Preparation of RNA-protein complexes for X-ray crystallography and NMR. In *RNA-Protein Interaction: Practical Approach*, Smith C (ed) pp 37-74. Oxford: Oxford University Press
- Sambrook J, Fritsch E & Maniatis T (1989) *Molecular Cloning: A Laboratory Manual*. Cold Spring Harbor Press, Cold Spring Harbor, New York, USA

Citations to manuscripts posted on recognized preprint servers can be cited the following way:

- Author NAME1, Author NAME2, (YEAR) article title. *bioRxiv* doi: 1234/002.dfj123 [PREPRINT]

Data citation

We encourage authors to include datasets obtained from public resources in the reference list in the form of data citations. Please note that a "dataset" in this context represents primary experimental data and *not* reference gene or protein sequences at public data banks such as Genbank, Ensembl or UniProt. The original publication (article) that reported the respective dataset should additionally be included as a regular reference.

Data references should include authors, when possible, the year, the full name of the database where the data is available, the accession number or DOI and, importantly, a resolvable link that points directly to the dataset. The resolvable link can be in the form of either a plain URL, a DOI or an identifiers.org construct. Each data reference should be labeled with the tag "[DATASET]" at the end to distinguish it from the other references. Example:

References

Hörnberg E, Ylitalo EB, Crnalic S, Antti H, Stattin P, Widmark A, Bergh A, Wikström P (2011) Gene Expression Omnibus GSE29650 (https://www.ncbi.nlm.nih.gov/geo/query/acc.cgi?acc=GSE29650). [DATASET]

Hörnberg E, Ylitalo EB, Crnalic S, Antti H, Stattin P, Widmark A, Bergh A, Wikström P (2011) Expression of androgen receptor splice variants in prostate cancer bone metastases is associated with castration-resistance and short survival. PLoS One

6: e19059

In the main text, these datasets should be cited with the prefix "Data ref:" to distinguish them from the reference to the original article that reported the dataset. Example:

> "…were grouped based on the relative levels of AR-Vs expressed, mainly AR-V7 (Hörnberg *et al*, 2011; Data ref: Hörnberg *et al*, 2011)."

Datasets for which the authors are unknown should be included at the end of the reference list in the form: [dataset title] [year] [database name and accession number] [resolvable link to the dataset] followed by the tag "[DATASET]" at the end. Example:

> Genetic variation in Kuusamo (2015) European Genome-Phenome Archive EGAS00001000020 (https://www.ebi.ac.uk/ega/studies/EGAS00001000020) [DATASET]

In the main text these datasets should be cited using the name of the database, its accession number and the year. Example:

> "… 402 genomes from the Kuusamo Project (Data ref: European Genome-phenome Archive EGAS00001000020, 2015) …"

In studies that make use of many (i.e. more than approx. 20) pre-existing datasets, it might not be practical or feasible to cite them individually. In this case, it is therefore acceptable to provide a separate data reference list in the form of an Expanded View Table which should be called out from Materials & Methods.

Tables

Tables should be provided in .doc or .xls format and need to be editable (no image files). They can be included at the bottom of the main manuscript file or be sent as separate files. Tables should be numbered consecutively with Arabic numerals (1, 2, 3, 4). Tables should be self-explanatory and include a brief descriptive title. Footnotes to tables indicated by lower-case superscript letters are acceptable, but they should not include extensive experimental detail.

Conventions and Abbreviations

In general, the journal follows conventions given in Scientific Style and Format: The CBE Manual for Authors, Editors and Publishers (1994) Cambridge University Press, Cambridge, UK, 6th edn. Please follow Chemical Abstracts and its indexes for chemical names. For guidance in the use of biochemical terminology follow the recommendations issued by the IUPAC-IUBMB Joint Commission on Biochemical Nomenclature. In general, genes and genotypes should be indicated in italics; proteins and phenotypes should not be italicized.

Authors should use approved gene and gene product nomenclature and apply the italicization and capitalization formatting as appropriate for each organism's standard nomenclature. Please consult the appropriate nomenclature databases for correct gene names and symbols. Some useful general resources are: Entrez Gene (http://www.ncbi.nlm.nih.gov/gene); UniProt (http://www.uniprot.org/).

Try to restrict the use of abbreviations to SI symbols (standard units of measurements) and those recommended by the International Union of Pure and Applied Chemistry (IUPAC). Abbreviations should be defined in brackets after their first mention in the text, not in a list of abbreviations. SI symbols and symbols of chemical elements may be used without definition in the body of the paper. Abbreviations of standard biochemical compounds, e.g. ATP, DNA, nucleotides in nucleic acids, and amino acids in proteins, need not be defined.

Figures

Figure Legends

Figure legends should contain sufficient information to allow the reader to follow the data presented without referring back to the text, but should not be redundant with the Results section. Each figure must contain a heading. All symbols and abbreviations used in the figure must be defined, unless they are common abbreviations or have already been defined in the text. Experimental details should, where possible, be given in the Materials and Methods section, and not repeated in the figure legends. Figure legends should be formatted such that each panel, or group of panels, has its own entry with the panel letter (or range) on the left and the description on the right, the panels should be described in sequential order in the legend. Details on the statistical analysis and the number of replicates should be indicated for each panel where appropriate (see Statistics section below).

Figure 1 - Generation of hiPSCs from a patient with type-2 long-QT syndrome.

A Bright-field images of neurospheres obtained from SVZ neural stem cells of P15 control and hGFAP-SDHD mouse brains. Scale bars: 500 μm.

B, C Neurosphere (NS) forming efficiency (B) and core diameter (C) in cultures grown from SVZ of P15 control and hGFAP-SDHD mice (n = 6 cultures/mice for each genotype).

D Quantitative RT–PCR detection of SdhD expression levels in SVZ neurospheres of wild-type (flox/+) and mutant (flox/-, and flox/- cre) mice (n = 4 mice for each group).

Data information: In (B–D), data are presented as mean ± SEM. *P≤0.05 (Student's t-test).

Figure Formatting

Figures and Expanded View figures should be presented in the order they are mentioned in the text. Figures use the numbering system **Fig 1**, while Expanded View figures use the system **Fig EV1**. The figure count in each is separate, such that there will be both a Fig 1 and a Fig EV1 (and so on) in a manuscript.

The final size of figures will be between 87 mm and 180 mm wide on the printed page. Please bear this in mind when submitting your manuscript for review and allow for sufficient resolution at a suitable size. For help preparing figures, please download our figure guide PDF.

Figures divided into parts should be labelled with an upper-case, bold letter (Helvetica Font). Figures with several parts should also be in proportion, with consistently sized lettering so that the whole figure can be reduced by the same amount to the smallest size at which the essential details are visible. Use Courier font for sequence data and Symbol font for any symbols.

All lettering should be done using standard fonts (Helvetica, Times, Symbol, Courier) and retained in a separate layer (if possible) so that the production team can adapt any labels to the journal's style if necessary. All fonts used for labelling the figures should also be embedded in the final files if the software package offers this option.

Scale bars, rather than magnification factors, should be used, with the length of the bar defined in the legend rather than on the bar itself. In general, visual cues on the figure itself are preferred rather than verbal explanations (for example, 'broken line' or 'filled black triangles') in the legend.

When preparing figures of microscopy images, please note that we strongly encourage the use of colours that are suitable for colour-blind readers: for example, the use of magenta/green is preferred over red/green for 2-channel images.

For publication, we require PowerPoint, TIFF, PDF or EPS files in PC or Macintosh format, preferably from PhotoShop or Illustrator software. We cannot accept Freehand, Canvas, CorelDRAW or MacDrawPro files. These files must be converted to postscript (eps) format. For any figures submitted in Photoshop or TIF(F) format we require layered files to be sent whereby all text, arrows or additional attributes are placed on individual layers within the file. For line art/charts/graphs we prefer to work with Adobe Illustrator AI, EPS or high-resolution PDF files. We can also accept high-resolution PDF files.

Colour artwork can be submitted in RGB or CMYK colour mode. Non-vector graphics should be preserved at high resolution: 300 ppi (pixels per inch) minimum at actual print size for greyscale or colour halftone images, and 600 ppi minimum for artwork containing fine details like lines and text. Combinations of monochrome line art (e.g. charts and diagrams) and greyscale/photographs should allow for a resolution of 600 ppi at the actual final print size.

An illustrated overview of the guidelines, explanations and tips regarding the preparation of artwork is available for download in this document [pdf].

The journal does not have colour charges for figures, and the authors are therefore welcome to submit full colour figures.

Figure/Data Presentation

Figures must accurately reflect the results of the experiments. Appropriate controls, markers and scale bars should be included in all panels. Statistical tests must be clearly defined and appropriate to the data.

Source Data
The EMBO Press journals strongly encourage authors to upload the ‘source data’ – for example, tables of individual numerical values and measurements or uncropped gels – that were used to generate figures. These files are separate from the Expanded View information files and are submitted using the "figure source data" option in the manuscript submission system. Source data are directly linked to specific figures so that interested readers can directly download the associated ‘source data’ for the purpose of alternative visualization, re-analysis or integration with other data.

The data should at minimum allow users to redraw the figures using an alternative graphical representation, or to identify how a gel was cropped or otherwise edited for inclusion in the original figure. The data should be annotated to provide essential information to interpret the source data.

Image Processing
Images submitted with a manuscript for review should be minimally processed (for instance, to add arrows to a micrograph). Authors should retain their unprocessed data and metadata files, as editors may request them to aid in manuscript evaluation. If unprocessed data are unavailable, manuscript evaluation may be stalled until the issue is resolved.

A certain degree of image processing is acceptable for publication (and for some experiments, fields and techniques is unavoidable), but the final image must correctly represent the original data and conform to community standards. The guidelines below will aid in accurate data presentation at the image processing level; authors must also take care to exercise prudence during data acquisition, where misrepresentation must equally be avoided. Where appropriate, manuscripts should include further Methods as part of the Expanded View that describe for each figure the pertinent instrument settings, acquisition conditions and processing changes.

Authors should list all image acquisition tools and image processing software packages used. Authors should document key image-gathering settings and processing manipulations in the Methods.

Images gathered at different times or from different locations should not be combined into a single image, unless it is stated that the resultant image is a product of time-averaged data or a time-lapse sequence. If juxtaposing images is essential, the borders should be clearly demarcated in the figure and described in the legend.

The use of touch-up tools, such as cloning and healing tools in Photoshop, or any feature that deliberately obscures manipulations, is to be avoided.

Processing (such as changing brightness and contrast) is appropriate only when it is applied equally across the entire image and is applied equally to controls. Contrast should not be adjusted so that data disappear. Excessive manipulations, such as processing to emphasize one region in the image at the expense of others (for example, through the use of a biased choice of threshold settings), is inappropriate, as is emphasizing experimental data relative to the control.

When submitting revised final figures upon conditional acceptance, authors may be asked to submit original, minimally processed images.

Electrophoretic gels and blots
Positive and negative controls, as well as molecular size markers, should be included on each gel and blot. For previously characterized antibodies, a citation must be provided. For antibodies less well characterized in the system under study, a detailed characterization that demonstrates not only the specificity of the antibody, but also the range of reactivity of the reagent in the assay, should be published as part of the Expanded View. The display of cropped gels and blots in the main paper is permitted if it improves the clarity and conciseness of the presentation. Cropped gels in the paper must retain all important bands, and space (several band-widths) should be retained above and below the relevant band(s). Vertically sliced images that juxtapose lanes that were non-adjacent in the gel must have a clear separation or a black line delineating the boundary between the gels. Quantitative comparisons between samples on different gels/blots are discouraged; if this is unavoidable, the figure legend must state that the samples derive from the same experiment and that gels/blots were processed in parallel. Loading controls must be run on the same blot. High-contrast gels and blots are discouraged, as overexposure may mask additional bands. Authors should strive for exposures with gray backgrounds. Multiple exposures should be presented in the Expanded View information if high contrast is unavoidable. Immunoblots should be surrounded by a black line to indicate the borders of the blot, if the background is faint. For quantitative comparisons, appropriate reagents, controls and imaging methods with linear signal ranges should be used.

Microscopy
Authors should be prepared to supply the editors with original data on request, at the resolution collected, from which their images were generated. Cells from multiple fields should not be juxtaposed in a single field; instead multiple supporting fields of cells should be shown as part of the Expanded View. Specific guidelines: Adjustments should be applied to the entire image. Threshold manipulation, expansion or contraction of signal ranges and the altering of high signals should be avoided. If 'Pseudo-colouring' and nonlinear adjustment (for example 'gamma changes') are used, this must be disclosed. Adjustments of individual colour channels are sometimes necessary on 'merged' images, but this should be noted in the figure legend. We encourage inclusion of the following with the final revised version of the manuscript for publication: In the Methods, specify the type of equipment (microscopes/objective lenses, cameras, detectors, filter model and batch number) and acquisition software used. Although we appreciate that there is some variation between instruments, equipment settings for critical measurements should also be listed. A further Methods section as part of the Expanded View (or part of a larger Methods section) titled 'equipment and settings' should list for each image: acquisition information, including time and space resolution data (xyzt and pixel dimensions); image bit depth; experimental conditions such as temperature and imaging medium; and fluorochromes (excitation and emission wavelengths or ranges, filters, dichroic beamsplitters, if any). The display lookup table (LUT) and the quantitative map between the LUT and the bitmap should be provided, especially when rainbow pseudocolor is used. If the LUT is linear and covers the full range of the data, that should be stated. Processing software should be named and manipulations indicated (such as type of deconvolution, three-dimensional reconstructions, surface and volume rendering, 'gamma changes', filtering, thresholding and projection). Authors should state the measured resolution at which an image was acquired and any downstream processing or averaging that enhances the resolution of the image.

Statistical analysis
The description of all reported data that includes statistical testing must state the name of the

statistical test used to generate error bars and P values, the number (n) of independent experiments underlying each data point (not replicate measures of one sample), and the actual P value for each test (not merely 'significant' or 'P < 0.05'). Discussion of statistical methodology can be reported in the materials and methods section, but figure legends should contain a basic description of n, P and the test applied.

Descriptive statistics should include a clearly labelled measure of centre (such as the mean or the median), and a clearly labelled measure of variability (such as standard deviation or range). Ranges are more appropriate than standard deviations or standard errors for small data sets. Standard error or confidence interval is appropriate to compare data to a control. Graphs must include clearly labelled error bars for cases where more than two independent experiments have been performed (error bars for replicate samples are less useful). Authors must state whether a number that follows the ± sign is a standard error (s.e.m.) or a standard deviation (s.d.) Authors must justify the use of a particular test and explain whether their data conform to the assumptions of the tests. In particular:

- When using statistical methods based on the normal distribution authors should explain how they tested their data for normality. If the data do not meet the assumptions of the test, then a non-parametric alternative should be used.
- When making multiple statistical comparisons on a single data set, authors should explain how they adjusted the alpha level to avoid an inflated Type I error rate, or they should select statistical tests appropriate for multiple groups.
- For each experiment, the number of both technical and biological replicates should be clearly stated. Biological replicates are derived from independent experiments using separately obtained biological samples, while technical replicates are created by repeated measurements on the same biological sample. In general, technical replicates should be averaged before any statistical inference tests are performed.
- In cases where n is small, appropriate statistical tests should be employed and justified in the text.

Since for complex biological experiments the number of independent repeats of a measurement often has to be limited for practical reasons, statistical measures with a very small n are commonplace. However, statistical measures applied to too small a sample size are not significant and they can suggest a false level of significance. We recommend that the actual individual data from each experiment should be plotted if n < 5, alongside an error bar. In cases where n is small, a justification for the use of the statistical test employed has to be provided. Presenting a single ‘typical result’ of n experiments is sometimes unavoidable, but should be accompanied by an indication of the variability of data between independent experiments. If n is not based on independent experiments (that is, n merely represents replicates of a measurement), statistics may still be useful, but a detailed description of the repeated measurement is required.

For more information on the appropriate use of standard deviation, standard error, and confidence intervals please refer to Sullivan et al (2016), American Statistical Association guidelines (2016), Motulsky (2014), and Cumming et al (2007).